2 Filter Basics

This chapter is devoted to fundamental filter concepts. A filter is a network, passive or active, which passes a desired set of frequencies, the passband, with a minimum of attenuation. Other frequencies, the stopband, are attenuated. Although the fundamental concepts presented are aimed primarily at the analysis and design of *LC* filters, they may be applied equally well to virtually any network. For example, the hybrid-pi bipolar transistor presented in the preceding chapter predicts a low-pass-filter–like response. The gain at low frequencies is high, but decreases with increasing frequency.

The early sections of this chapter are introductory and are intended primarily as a review. These sections are, nonetheless, very important, for they emphasize the dual methods used for network analysis. Either time or frequency may be used as the independent controlling variable. Once an analysis has been done with respect to frequency (in the frequency domain), the circuit performance with respect to time (in the time domain) is also determined. The two domains are related by Fourier or Laplace transforms.

Filters are traditionally characterized in the frequency domain. That is, they may be low pass or bandpass circuits. Time domain behavior has been analyzed, but is often ignored in the design process. It is becoming increasingly important to design filters with a desired time domain characteristic in addition to a suitable frequency response. This is especially critical in modern digital communications systems and in rf instrumentation.

The later part of this chapter deals primarily with low pass filters. The methods presented are extended to the design of simple high pass and bandpass networks.

Chapter 3 is an extension which treats a filter of special interest to the rf designer, the coupled resonator bandpass.

2.1 NETWORK ANALYSIS IN THE TIME DOMAIN

The traditional method for network analysis is with differential equations with time as the independent variable. This is illustrated in this section with a number of simple circuits. The reader is assumed to have a background in differential equations and a familiarity with ac circuit theory. Some texts written specifically for the study of electronic networks will supply both backgrounds. Especially recommended are the fundamental volumes by Van Valkenburg (1) and Skilling (2). The more advanced reader is directed toward the outstanding text by Blinchikoff and Zverev (3).

The first circuit considered is a constant voltage applied to an RC network, Fig. 2.1. The switch is assumed closed until $t = 0$ when it is opened. The charge on the capacitor is related to the voltage by $Q = CV$. But current is the time rate of change of charge. Hence

$$V = \frac{1}{C}\int I\,dt \tag{2.1-1}$$

We use Kirchhoff's voltage law to write an equation to describe the total voltage drop in the circuit

$$V = IR + \frac{1}{C}\int I\,dt \tag{2.1-2}$$

The equation is differentiated and divided by the resistance

$$\frac{dI}{dt} + \frac{1}{RC}I = 0 \tag{2.1-3}$$

The equation is multiplied by an integrating factor, $e^{t/\tau}$, where $\tau = RC$,

$$\frac{dI}{dt}e^{t/\tau} + \frac{I}{\tau}e^{t/\tau} = 0 \tag{2.1-4}$$

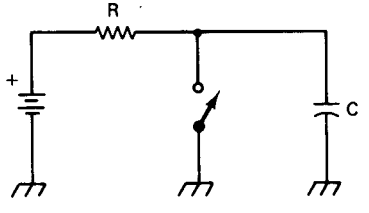

Figure 2.1 Simple resistor-capacitor circuit with a dc drive.

Recalling the rule for differentiation of a product, this reduces to

$$\frac{d}{dt}(Ie^{t/\tau}) = 0 \tag{2.1-5}$$

Direct integrations yields

$$Ie^{t/\tau} = K \tag{2.1-6}$$

where K is a constant of integration, evaluated from initial conditions. The current prior to opening the switch was V/R. It must be the same just after the switch is opened, for the voltage across the capacitor cannot change instantaneously. The final solution is the familiar decreasing exponential

$$I(t) = \frac{V}{R} e^{-t/\tau} \tag{2.1-7}$$

The capacitor voltage is obtained from direct application of Kirchhoff's voltage law.

A similar equation will describe application of a dc voltage to an LR circuit, as shown in Fig. 2.2. The circuit is assumed to be initially in a relaxed condition with no current flowing. The switch is changed at $t = 0$. The differential equation is written directly, noting that the voltage drop across L is $L(dI/dt)$

$$V = L\frac{dI}{dt} + IR \tag{2.1-8}$$

This is divided by L and multiplied by the integrating factor, $e^{t/\tau}$, to yield

$$\frac{V}{L} e^{t/\tau} = \frac{dI}{dt} e^{t/\tau} + \frac{I}{\tau} e^{t/\tau} \tag{2.1-9}$$

where $\tau = L/R$. Integration and subsequent division by the integrating factor produces

$$I = \frac{V}{R} + Ke^{-t/\tau} \tag{2.1-10}$$

The constant of integration, K, is evaluated from initial conditions. $I = 0$ at $t = 0$, for the current in an inductor cannot change instantaneously. The inductor is the dual of the capacitor which inhibits an instantaneous voltage change. The final solution is

$$I(t) = \frac{V}{R}(1 - e^{-t/\tau}) \tag{2.1-11}$$

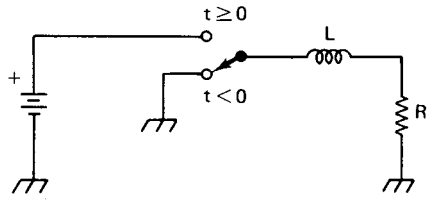

Figure 2.2 Inductor-resistor circuit with dc step input.

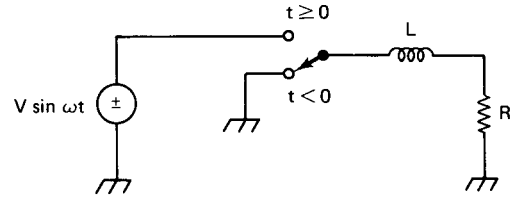

Figure 2.3 Inductor-resistor network with a sinusoidal input.

A more interesting circuit for the rf engineer is one where the dc voltage is replaced with a sinusoidal source. This is shown in Fig. 2.3 and is described by

$$V \sin \omega t = L\frac{dI}{dt} + IR \tag{2.1-12}$$

Application of an integrating factor produces

$$\frac{d}{dt}(Ie^{t/\tau}) = \frac{V}{L} e^{t/\tau} \sin \omega t \tag{2.1-13}$$

Integration and manipulation yield

$$I(t) = \frac{\dfrac{V}{L}\dfrac{1}{\tau} \sin \omega t - \omega \cos \omega t}{\dfrac{1}{\tau^2} + \omega^2} + Ke^{-t/\tau} \tag{2.1-14}$$

The second term vanishes in time and is ignored in this analysis. The first term is simplified by the substitutions

$$\begin{aligned} \frac{1}{\tau} &= K' \cos \phi \\ -\omega &= K' \sin \phi \end{aligned} \tag{2.1-15}$$

producing a familiar trigonometric form

$$K' \cos \phi \sin \omega t + K' \sin \phi \cos \omega t = K' \sin (\omega t + \phi) \tag{2.1-16}$$

The angle, ϕ, is evaluated as

$$\tan \phi = \frac{\sin \phi}{\cos \phi} = \frac{-\omega/K'}{1/(K'\tau)} = \frac{-\omega L}{R} \tag{2.1-17}$$

K' is evaluated with the identity $\sin^2 \phi + \cos^2 \phi = 1$. The final steady state current is

$$I_{ss}(t) = \frac{V \sin(\omega t + \phi)}{(\omega^2 L^2 + R^2)^{1/2}} \tag{2.1-18}$$

These results are interpreted by allowing individual components to become small. As L vanishes, I_{ss} becomes the ratio of the ac voltage to the resistance, Ohm's law. Current is in phase with the driving voltage source. If the resistance vanishes, I_{ss} becomes the driving current and is divided by ωL. The tangent of the phase angle becomes infinite, indicating a 90 degree phase difference between the voltage and the current. Intermediate values of L and R produce phase differences between 0 and 90 degrees. The denominator of Eq. 2.1-18 is termed the impedance of the network.

Equation 2.1-18 is termed a transfer function in the time domain if V is set to unity. It is a transfer admittance here, for it is the output current, $I_{ss}(t)$, per unit input voltage. The related output voltage across R of Fig. 2.3 is easily calculated. This results in a voltage transfer function if $V = 1$.

A similar result will be obtained if the RC network (Fig. 2.1) is driven from a sinusoidal voltage source. The inductive term, ωL, is replaced with $1/(\omega C)$ and the phase angle has the opposite sign.

The steady state ac current is the driving voltage divided by a suitable impedance, a characteristic of the network and not of the driving signal.

These methods are easily extended to more complicated networks with many more components. The differential equations become predictably more complicated although the methods for solution are similar.

2.2 NETWORK ANALYSIS IN THE FREQUENCY DOMAIN

Previous circuits were analyzed with time as the independent variable. This traditional approach is reasonable. Length, mass, and time are the three basic units of physics from which all others are derived. Time forms a natural basis for circuit description by differential equations.

A duality is observed when many circuits are analyzed. The frequency dependence is often mathematically similar to the time dependence. It is then natural to examine methods that will emphasize the frequency dependence of a function of time.

Numerous techniques exist to assess the frequency content of a time function. Any periodic function may be expanded in a Fourier series. An example was considered in the previous chapter.

An arbitrary function of time, not necessarily periodic, is transformed to a function only of frequency by the Fourier transform

$$F(\omega) = \int_{-\infty}^{\infty} F(t) e^{-j\omega t} dt \tag{2.2-1}$$

The integration removes all time dependence from the result.

A function of frequency is similarly transformed into a time dependent one with the inverse Fourier transform

$$F(t) = \frac{1}{2\pi} \int_{-\infty}^{\infty} F(\omega) e^{j\omega t} \, d\omega \tag{2.2-2}$$

These transforms are very useful for many electronics applications. However, they are not well suited to the solution of differential equations. The transforms do not exist for all functions. A better transformation is sought.

Section 2.1 gave the results of RC and RL networks when driven by a dc source. More explicitly, the drive was the unit step function, $u_{-1}(t)$, formally 0 for $t < 0$ and 1 for $t \geq 0$. The results for the networks considered were decreasing exponential time functions. Any transformation that might be picked for analysis should apply well to the unit step. The transformation should, ideally, have physical significance for any arbitrary driving function including a sinusoid.

The desired transformation is the Laplace transform, defined as

$$F(s) = \mathcal{L} f(t) = \int_{0}^{\infty} f(t) e^{-st} \, dt \tag{2.2-3}$$

where $f(t)$ is the time domain function and e^{-st} is the multiplying factor. s is the so-called Laplace frequency, and is defined by

$$s = \sigma + j\omega \tag{2.2-4}$$

This frequency can be real, imaginary, or complex. Many functions that are not integrable alone, or are not Fourier transformable, have Laplace transforms. This is a result of the $e^{-\sigma t}$ component of e^{-st} which forces the integral to converge at large t. Note that the Laplace transform is dependent on the values of the time function only at times in the future. Earlier history is of no significance as it was for the Fourier transform. Capital letters are used to represent the transformed functions. Hence, $F(s)$ is the transformed, frequency domain version of the time domain function $f(t)$.

There are many details of the Laplace transformation that are both of scholarly interest and vital to its application. These are found in many texts including those referenced earlier. They are not presented here, for our goal is to gain intuition about a specific application, filter design.

The greatest virtue of the Laplace transformation to the electronic designer is the simplicity it affords. It will allow us to study problems directly in the frequency domain. Analysis will be through straightforward algebraic manipulation to yield $F(s)$, the frequency domain solution. The corresponding time function, $f(t)$, is found from the inverse transformation, or from a search of tables of Laplace transforms.

There are two functions of special significance in interpretation of $F(s)$. One is the unit impulse, or Dirac delta function, $\delta(t - x)$. It is zero for all values of

time except $t = x$ where it is unbounded. However, it is infinite in a special way such that its integral is unity. In the strictest sense, the unit impulse has significance only when it appears within an integral. As such, it is often termed a functional (4). The Laplace transform of the unit impulse is unity, shown by direct integration.

The other vital function is the unit step, $u_{-1}(t)$, defined earlier. The Laplace transform of the unit step is $1/s$.

The key to application of the Laplace transform in electronics lies in the frequency domain transfer function, $H(s)$. Time domain transfer functions were discussed in the previous section for the case of sinusoidal excitation.

$H(s)$ is written directly in the frequency domain for practical networks through application of Kirchhoff's laws. The impedance of an inductor was shown earlier to be $j\omega L$. In the frequency domain, the impedance is $Z_L(s) = sL$. Similarly, the impedance of a capacitor is $Z_C(s) = 1/sC$. A resistor has an impedance of R in both domains. Examples of $H(s)$ will be presented below.

The casual designer will often use s, the complex frequency, merely as a shorthand notation for $j\omega$. This is valid to the extent that it provides proper results. It is, however, a severely restricted interpretation of Laplace methods. A more general and significantly more profound result is

$$F_{out}(s) = H(s)F_{in}(s) \tag{2.2-5}$$

Once $H(s)$ is known, the frequency domain output is known for any arbitrary input function, $F_{in}(s)$, so long as that input function is Laplace transformable.

Recall that the transform of the impulse function was unity. $H(s)$ is then the frequency domain impulse response. Similarly, $u_{-1}(t) = 1/s$. Hence, $(1/s)H(s)$ is the frequency domain response to a step function. Either result is obtained in the time domain with an inverse transformation of the frequency domain calculation.

The response to a sinusoidal excitation is obtained by a direct substitution of $j\omega$ for s in $H(s)$. The result is called the frequency response of the network.

The simplicity and elegance of the Laplace methods are illustrated with an example, the LR circuit analyzed earlier with traditional methods. The circuit is repeated in Fig. 2.4, now with an arbitrary input driving function. The frequency domain impedance of the network is $R + sL$. Hence, the current transfer function is

$$H(s) = \frac{1}{R + sL} \tag{2.2-6}$$

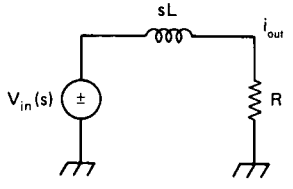

Figure 2.4 Inductor-resistor network with an arbitrary input voltage.

The frequency response is evaluated initially with direct substitution of $j\omega$ for s

$$H(j\omega) = \frac{1}{R + j\omega L} \tag{2.2-7}$$

If the input is a voltage at a frequency ω, $V \sin \omega t$, the time domain current is

$$I(t) = \frac{V \sin \omega t}{R + j\omega L} \tag{2.2-8}$$

or

$$I_{out}(t) = \frac{V \sin (\omega t + \phi)}{(R^2 + \omega^2 L^2)^{1/2}} \tag{2.2-9}$$

where $\phi = \tan^{-1}(\omega L/R)$. This is identical to the previous steady state response.

The impulse response is evaluated by obtaining the inverse transform of $H(s)$. A tabulation of Laplace transforms shows that the corresponding time domain function is $e^{-t/\tau}$ where $\tau = L/R$.

Dividing $H(s)$ by s yields the response to a unit step input. This is transformed, again from perusal of a tabulation of Laplace transforms, to

$$I_{out}(t) = \frac{1}{R}(1 - e^{-t/\tau}) \tag{2.2-10}$$

Again, this is identical with the earlier result with a driving voltage of $V = 1$. The analysis is easier with Laplace methods and provides considerably more information.

2.3 POLES, ZEROS, AND THE SERIES TUNED CIRCUIT

The next example is the familiar series resonant circuit. This is of importance unto itself and will further illustrate the utility of the Laplace method. The concept of complex frequency will be presented in more detail in connection with the circuit.

The series tuned circuit is shown in Fig. 2.5. The total impedance of the network

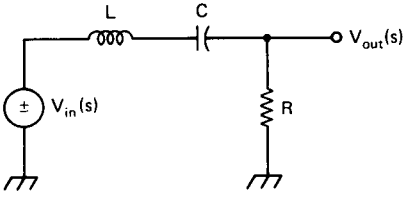

Figure 2.5 Series tuned circuit with arbitrary frequency domain drive.

is $sL + 1/(sC) + R$. Noting the voltage divider action, the frequency domain voltage transfer function is

$$H(s) = \frac{R}{sL + \frac{1}{sC} + R} = \frac{sCR}{s^2LC + 1 + sCR} \tag{2.3-1}$$

The usual substitutions are defined

$$\omega_0^2 = \frac{1}{LC} \qquad \frac{\omega_0 L}{R} = Q \tag{2.3-2}$$

$H(s)$ then becomes

$$H(s) = \frac{s/(\omega_0 Q)}{s^2/\omega_0^2 + 1 + s/(\omega_0 Q)} \tag{2.3-3}$$

The steady state frequency response is first evaluated. Replacement of s by $j\omega$ yields

$$H(j\omega) = \frac{j\omega/(\omega_0 Q)}{1 - (\omega/\omega_0)^2 + j\omega/(\omega_0 Q)} \tag{2.3-4}$$

Consider the limiting cases. The denominator of $H(j\omega)$ approaches unity at very low frequencies, while the numerator vanishes. Hence, the frequency response goes toward zero. At $\omega = \omega_0$, $H(j\omega)$ reduces to unity. The response again starts to decrease as the frequency continues to increase, going to zero at very high frequencies. This may be confirmed through detailed calculation, but is generally clear from inspection. The numerator and denominator both increase with frequency. However, the quadratic term in the denominator causes it to dominate.

The inductive reactance equals the reactance of the capacitor at a radial frequency of $\omega = \omega_0$, and f_0 is defined as the resonant frequency where $\omega_0 = 2\pi f_0$. The transfer function is maximum at this frequency because the impedances of the inductor and capacitor, while equal in magnitude, have opposite signs.

The parameter Q was introduced in Eq. 2.3-2. The effect of various Q values is shown in Fig. 2.6. Figure 2.6a shows the relative amplitude plotted on a logarithmic scale while Fig. 2.6b shows the phase response. Curves are presented for $Q = ½$, 2, and 6.

A number of features of Fig. 2.6 deserve further comment. The curves are not symmetrical about the center frequency, $\omega/\omega_0 = 1$. (They would be symmetrical if the method of graphing had been changed.) The phase changes more rapidly near resonance with higher Q. The phase is + and −45 degrees at the points where the amplitude response is down by 3 dB. Similar results may be obtained for other phases

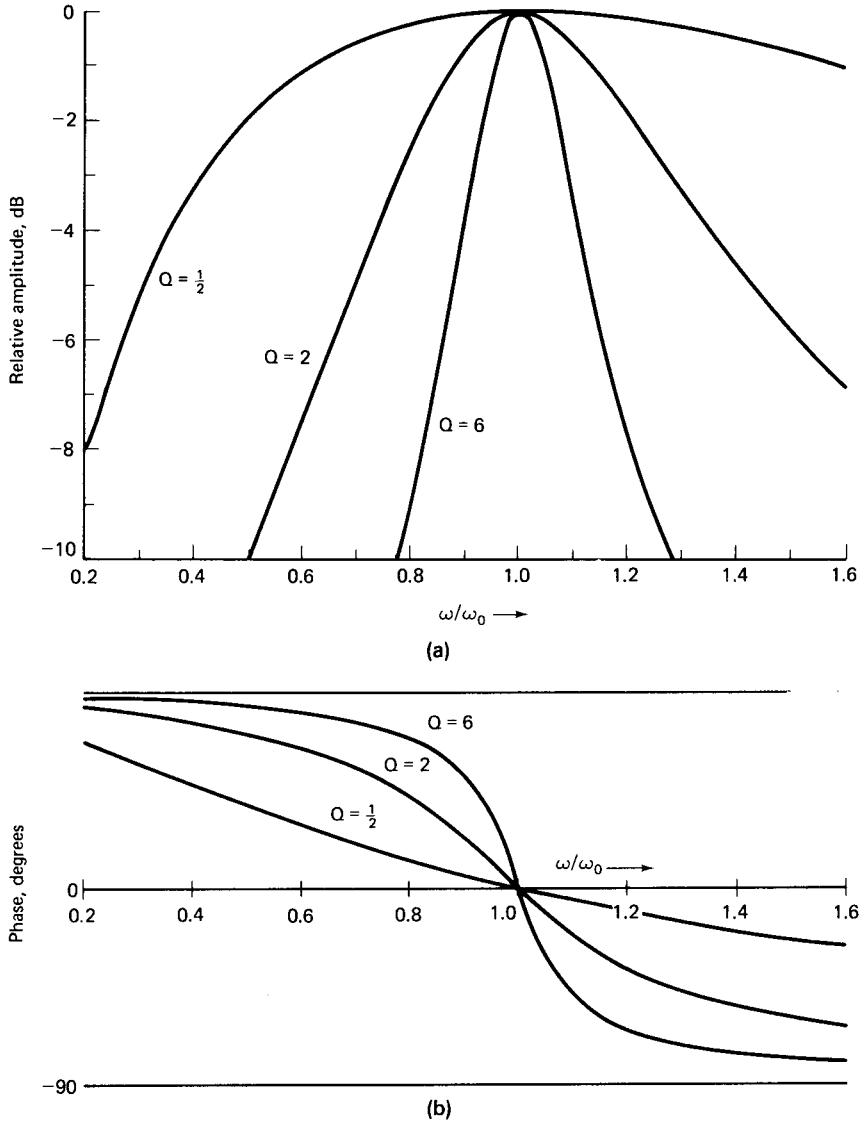

Figure 2.6 Frequency response (a) and phase response (b) for the series tuned circuit with $Q = \frac{1}{2}$, 2, and 6.

and attenuations. This is an example of a more general observation that phase and amplitude responses are not independent of each other. Not all networks have this characteristic, but many do.

Returning to the transfer function, $H(s)$, Eq. 2.3-1, we see that the Laplace frequency s appears in both the numerator and denominator. Generally, the transfer function of an arbitrary linear network is of the form

$$H(s) = \frac{P(s)}{Q(s)} = \frac{b_0 + b_1 s + \cdots + b_m s^m}{a_0 + a_1 s + \cdots + a_m s^m} \tag{2.3-5}$$

The transfer function is a ratio of two polynomials in s, the Laplace frequency. The highest power of the denominator polynomial equals the number of reactive elements in the network. The numerator polynomial will have an order that is less than or equal to that of the denominator with the former being more common. The polynomials may be factored to

$$H(s) = K \frac{(s - z_1)(s - z_2) \cdots (s - z_m)}{(s - p_1)(s - p_2) \cdots (s - p_n)} \tag{2.3-6}$$

where K is a scalar constant. The numerator vanishes at a complex frequency $s = z_m$. Such a complex frequency is termed a zero of the function. Similarly, at $s = p_n$, the denominator vanishes, causing the transfer function to become infinite. Such a complex frequency is termed a pole of the transfer function.

The transfer function of the series tuned circuit, Eq. 2.3-1, is clearly the ratio of two polynomials. The numerator has no constant frequency independent terms. Hence, the zero occurs at $s = 0$. Recall that the poles and zeros are complex frequencies, $s = \sigma + j\omega$. While the resonant frequency, f_0, might be considered a "natural" frequency of the network, the more significant natural frequencies are the poles and zeros. The frequency response, $H(j\omega)$, occurs not from excitation of the network at a natural frequency, but for a complex frequency with only an imaginary part, $j\omega$.

The denominator of the series tuned circuit transfer function is factored using the quadratic formula

$$p_{1,2} = \frac{-\omega_0}{2Q} [1 \pm (1 - 4Q^2)^{1/2}] \tag{2.3-7}$$

The part of this function under the radical is positive if Q is less than ½. The roots will be real and negative. At $Q = ½$, the two roots are identical and have a magnitude of ω_0. The roots become complex for $Q > ½$. The roots are predominantly imaginary at high Q values.

It is useful to plot the position of the poles and zeros of a transfer function in the s plane. Such a plot for the double tuned circuit is shown in Fig. 2.7. Poles are plotted with an X while zeros are shown as a circle. Figure 2-7a shows a case of low Q where both roots are real. The poles lie on the negative real axis. The second part of the figure shows a case of $Q > ½$. The poles are now complex and lie on the circle centered at the origin with radius ω_0. The roots are almost at the imaginary axis with large Q. Note that the roots occur as complex conjugates.

The polynomials are usually much more difficult to factor for the general case, Eq. 2.3-5. A number of methods are available. They are presented in the literature. These range from careful algebra to numerical techniques.

Further meaning of the pole locations is gained from an analysis of the step

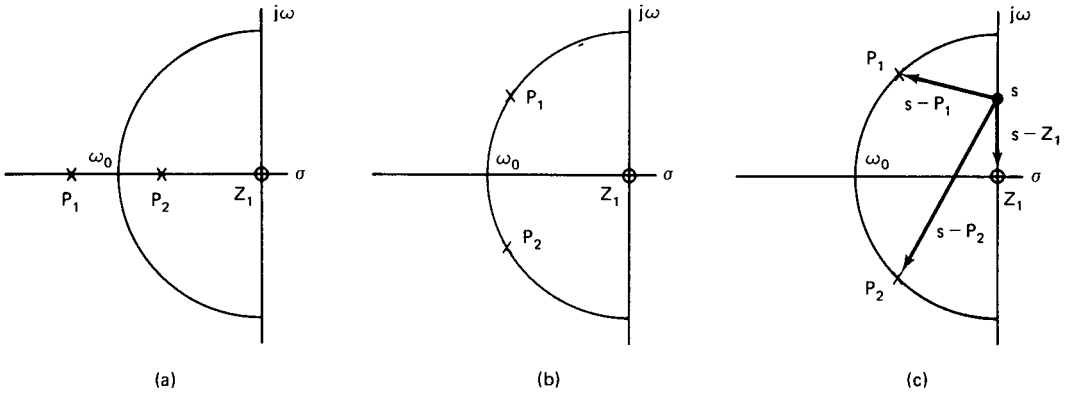

Figure 2.7 Pole-zero plots for the series tuned circuit of Fig. 2.5. (a) shows a low Q example while a higher Q occurs at (b). (c) shows the method of using vectors with a pole-zero diagram to infer network response.

response of the single tuned circuit. Dividing $H(s)$ by s yields the step response in the frequency domain

$$V_0(s) = \frac{1/(\omega_0 Q)}{\frac{s^2}{\omega_0^2} + 1 + \frac{s}{\omega_0 Q}} \tag{2.3-8}$$

The denominator has already been factored with known pole locations. A table of Laplace transforms shows

$$\mathcal{L}\frac{1}{a-b}(e^{at} - e^{-bt}) = \frac{1}{(s-a)(s-b)} \tag{2.3-9}$$

which leads to the time domain step response

$$V_0(t) = \frac{1/(\omega_0 Q)}{p_1 - p_2}[\exp(p_1 t) - \exp(p_2 t)] \tag{2.3-10}$$

The real part of the exponential functions may be factored from the expression. The imaginary parts are decomposed to a sine function through Euler's identity with the final result for the step response

$$V_0(t) = \frac{2}{\omega_0^2} \frac{\exp(-\omega_0 t/2Q)\sin[(\omega_0/2Q)(4Q^2-1)^{1/2}t]}{(4Q^2-1)^{1/2}} \tag{2.3-11}$$

This is a sinusoidal oscillation multiplied by a decreasing exponential. It is said to be damped. The frequency of the sine component is less than ω_0 for small Q. The frequency approaches ω_0 as Q becomes large. In addition, the multiplying

part in the real exponential component, the damping term, becomes smaller. Hence, it will take longer for the "ringing" to damp to no perceptible signal after application of the step.

The real exponential function has a negative real exponent. The plot of pole location in the s plane, Fig. 2.7, is in the left half plane. A step input leads to an exponentially growing amplitude if a pole occurs in the right half plane. This is generally avoided with most circuits, for it represents an unstable condition.

A pole-zero plot such as the s-plane graphs of Fig. 2.7 are of great utility in graphical analysis. The series tuned circuit has a transfer function of the form

$$H(s) = \frac{(s - z_1)}{(s - p_1)(s - p_2)} \tag{2.3-12}$$

where the zero is at the origin, $z_1 = 0 + j0$. If excitation is considered at an arbitrary frequency s, each of the three terms in Eq. 2.3-12 is a vector. An example is shown in Fig. 2.7c where the frequency is a sinusoid and, hence, on the $j\omega$ axis. The magnitude of the frequency response ($s = j\omega$) is proportional to the length of the $(s - z_1)$ vector and inversely proportional to the magnitude of both of the $(s - p_n)$ vectors. The lengths may be measured graphically to infer the response of the network. Similarly, the angles of the individual vectors may be added or subtracted to evaluate the phase response.

The example shown in Fig. 2.7c is for an excitation frequency close to the resonant point, $\omega = \omega_o$. The $(s - z_1)$ and $(s - p_1)$ vectors have approximately the same length, so their ratio is unity. The $(s - p_2)$ vector is longer, so it diminishes the magnitude of the response accordingly.

An excitation frequency close to zero would produce a much different result. The two pole vectors would be of approximately equal length. The $(s - z_1)$ vector is very short, leading to a low output.

If the other extreme is considered, a very high input frequency, the zero vector will effectively cancel with one of the pole vectors. The other pole vector will then dominate. The long length will lead to a small network response.

Pole-zero plots are especially useful for quick graphical analysis of many networks and the subject is covered in many texts. The reader is encouraged to study the methods (5).

Pole-zero plots are equally useful for analysis of active networks. A transistor, modeled at high frequency, will contain reactive terms. These cause poles and zeros to arise in the frequency domain response. The complete amplifier is then characterized by $H(s)$.

2.4 FILTER CONCEPTS

Having acquired some basic tools for analysis, we will now investigate some of the basic filter structures. Figure 2.8 shows several idealized frequency responses.

The idealized low pass filter is shown in Fig. 2.8a. Frequencies below the cutoff

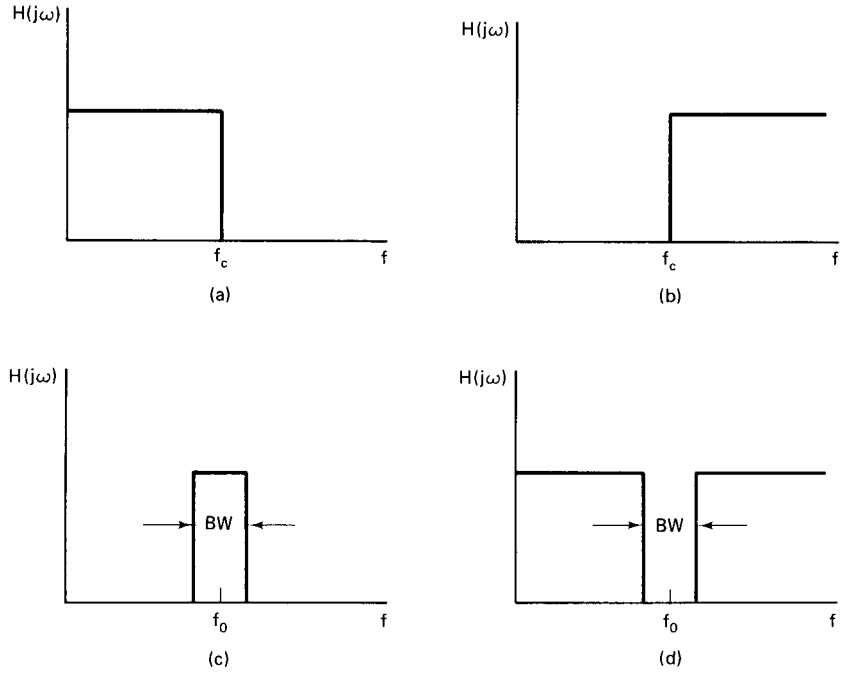

Figure 2.8 Idealized responses for (a) a low pass filter, (b) a high pass filter, (c) a bandpass filter, and (d) a bandstop filter.

frequency, f_c, are transferred through the filter without attenuation. This region is the passband. Frequencies greater than the cutoff are completely attenuated. This region is known as the stopband.

The high pass filter is the opposite of the low pass. Frequencies above the cutoff frequency are passed without attenuation while lower ones are attenuated.

An ideal bandpass filter is presented in Fig. 2.8c. The filter is centered about a frequency f_o, and has a bandwidth shown as BW in the figure. We have already seen one example of a bandpass filter, the single tuned circuit. It was, however, far from ideal.

Finally, Fig. 2.8d shows a bandstop filter. Frequencies outside of the bandwidth of the filter are passed without attenuation. Frequencies within the bandwidth are eliminated from the output.

A final filter type not shown in the figure is the all-pass structure. It passes all frequencies without attenuation. The utility of the all pass is that even though it shows no attenuation, it will shift the phase of signals passing through it. This is of value in numerous applications. One example of an all-pass filter is a matched transmission line.

The high pass and bandpass filters are designed from a low pass prototype filter through suitable transformations. These details will be presented subsequently. First some simple examples will be considered.

Figure 2-9 shows two simple networks. Each contains a resistor and one reactive

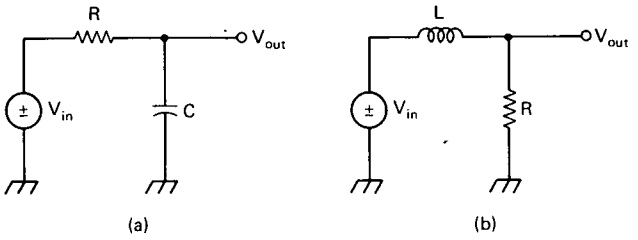

Figure 2.9 Simple low pass filters, each with one reactive element.

element. The frequency domain transfer functions are written using the s plane impedances and by noting the voltage divider action. $H(s)$ for the network with the capacitor, Fig. 2.9a, is

$$H(s) = \frac{1/sC}{R + 1/sC} = \frac{1}{1 + sCR} \tag{2.4-1}$$

This filter has a single pole in the s plane at $s = -1/RC$. The filter has no finite zeros. Substitution of $j\omega$ for s in Eq. 2.4-1 provides the frequency response. The filter shows no attenuation at dc. As frequency increases, the response immediately begins to decrease. This is clearly a low pass filter.

The network with the series inductor has a transfer function, $H(s)$

$$H(s) = \frac{R}{sL + R} = \frac{1}{1 + \dfrac{sL}{R}} \tag{2.4-2}$$

This filter has a single real pole at $s = -R/L$. Evaluation of the frequency response is similar to that of the capacitive filter. The inductor presents no impedance at dc; hence the filter has no attenuation. As the frequency increases so does the inductive reactance, leading to increasing attenuation. A low pass response arises.

For both low pass filters, the frequency response is below the dc value by a numerical factor of $1/\sqrt{2}$ at a radian frequency equal to the pole location. The power out of the filter is reduced by the square of this amount to ½. Taking the log of the power ratio and multiplying by 10 shows that the response is down by 3.01 dB, essentially 3 dB. This is defined as the cutoff frequency. The phase of the output then differs from the drive by 45 degrees in each filter.

Neither of the filters has a well-defined stopband. That is, there is never a finite frequency where the attenuation is infinite. This is true of virtually any real filter. The amount of attenuation required in a given application will define what the "stopband" of a filter will actually be. The slope of the response at frequencies well above the cutoff is 6 dB per octave, or 20 dB per decade, for both of the single-pole, low pass filters of Fig. 2.9. The phase of the response is −90 degrees when high frequencies are reached.

Figure 2.10 shows two additional filters. From inspection, we see that they

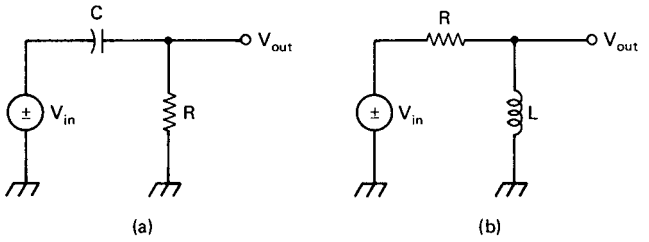

Figure 2.10 Simple high pass filters with (a) a series capacitor and (b) a shunt inductor.

are high pass structures. The capacitor in Fig. 2.10a is an open circuit at dc, producing infinite attenuation there. Similarly, the inductor (Fig. 2.10b) is a short at dc. The frequency domain transfer functions are

$$H(s) = \frac{sCR}{1 + sCR} \tag{2.4-3}$$

for the capacitive high pass filter and

$$H(s) = \frac{s}{s + R/L} \tag{2.4-4}$$

for the inductive example. The filters each have a single pole. They also exhibit a zero at the origin of the s plane. The 3-dB points occur for a radian frequency, ω_c, equal to the magnitude of the pole location. The slope is also 6 dB per octave at low frequencies. The phase is +90 degrees at very low frequencies with respect to the cutoff and is +45 degrees at the cutoff.

We have found from the foregoing discussion that low pass characteristics result from series inductors or shunt capacitors. Shunt inductors and series capacitors lead to high pass behavior. We can use this to form more elaborate filters. One example already covered is the series tuned circuit of the last section. An element of each type was placed in the series arm of the filter resulting in a bandpass characteristic. A number of low pass elements may additionally be cascaded to form a more exotic low pass structure. This also applies, of course, to the high pass.

Note that adding two reactances of the same type in the series arm of a filter will not change the general characteristic. For example, two series inductors will act as one inductor. This will lower the cutoff frequency, but will otherwise not alter the response. If a composite filter is to be formed, it must be done by mixing component types.

An example of a composite low pass filter is presented in Fig. 2.11. This filter is doubly terminated. That is, it has a driving source that is not a pure voltage generator, but one with an internal resistance, R_s. The output is terminated in a load resistance, R_L.

The frequency domain transfer function for the filter may be written from inspection, noting the voltage divider action of the composite network. An admittance, Y,

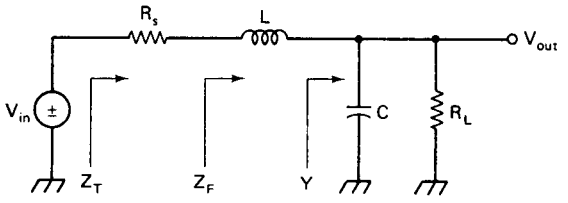

Figure 2.11 A two-pole, doubly terminated low pass filter.

is marked in Fig. 2.11. This is the admittance of the output load resistor in parallel with the capacitor, $Y = 1/R_L + sC$. The impedance of this combination is the reciprocal of the admittance, $Z = R_L(1 + sCR_L)^{-1}$. The total impedance looking in from the voltage generator is $Z_T = Z + R_s + sL$. The transfer function is thus

$$H(s) = \frac{Z}{Z_T} = \frac{1}{s^2LC + s\left(RC + \frac{L}{R}\right) + 2} \tag{2.4-5}$$

where $R_s = R_L = R$.

This filter has no finite zeros, but has two poles. They are evaluated by factoring the denominator polynomial of $H(s)$. The result is

$$P_{1,2} = \frac{-(RC + L/R) \pm [(RC + L/R) - 8LC]^{1/2}}{2LC} \tag{2.4-6}$$

If we allow the source and load resistances to be equal at 1 Ω and assign values of $L = \sqrt{2}$ henry (H) and $C = \sqrt{2}$ farad (F), the poles occur at $p = (1 \pm j1)/\sqrt{2}$.

We will examine the nature of impedance matching when reactive terminations are present before evaluation of the steady state frequency response. Maximum power transfer occurs from a source with characteristic resistance R_s when the load has the same value, $R_L = R_s$. However, this is not the proper condition when the source is a complex impedance.

Assume that the driving generator has a source resistance R_s in series with an inductor. The source impedance at a given angular frequency, ω, is $Z_s = R_s + j\omega L$. If a similar impedance was used as the load, the power transferred to the load is clearly not maximum. If the inductor in the load was removed, the net impedance would decrease, causing an increase in current. Hence, additional power would be dissipated in the load resistor. It is only the power in the resistor that is of significance. The voltage drop in the inductor is always 90 degrees out of phase with the current, leading to no power dissipation.

We ask what the source impedance should be for maximum power delivered to the load. The load would be one with the same resistance as that of the source, with a reactance opposite in sign, but with the same magnitude of the inductor. This reactance is, of course, a capacitor. The combination of inductor and capacitor would form a series resonant circuit. The total reactive impedance is zero. Neither

reactive component impedes the flow of current. In the general case, maximum power transfer occurs where the load impedance is the complex conjugate of the source impedance. This is termed a *conjugate match.*

Returning now to the filter of Fig. 2.11, the effective frequency response may be evaluated. We could insert $j\omega$ into Eq. 2.4-5 to obtain the response as was done in earlier examples. This would not be the most useful information though. It is more viable to consider the transducer gain of the filter. Recall that transducer gain was defined as the power delivered to the output termination divided by the available power from the generator.

The frequency response is written directly as

$$H(j\omega) = \frac{1}{(2 - 2\omega^2) + j\omega 2\sqrt{2}} \tag{2.4-7}$$

This will be the output voltage for an input of 1 V. Assume that the input is 2 V. Then, the output voltage is $H(j\omega)$ of Eq. 2.4-7 multiplied by 2. The maximum power available from the generator is half of the open circuit voltage across a load equal to the source impedance, or $P_A = 1/R_s$. The equation provides the output voltage, V_{out}. The output power is then V_{out}^2/R_L. Hence, transducer gain is $R_s V_{out}^2/R_L$. We will use this definition for filter frequency response throughout the rest of the text.

The frequency response of the filter is presented in Fig. 2.12 for the filter of

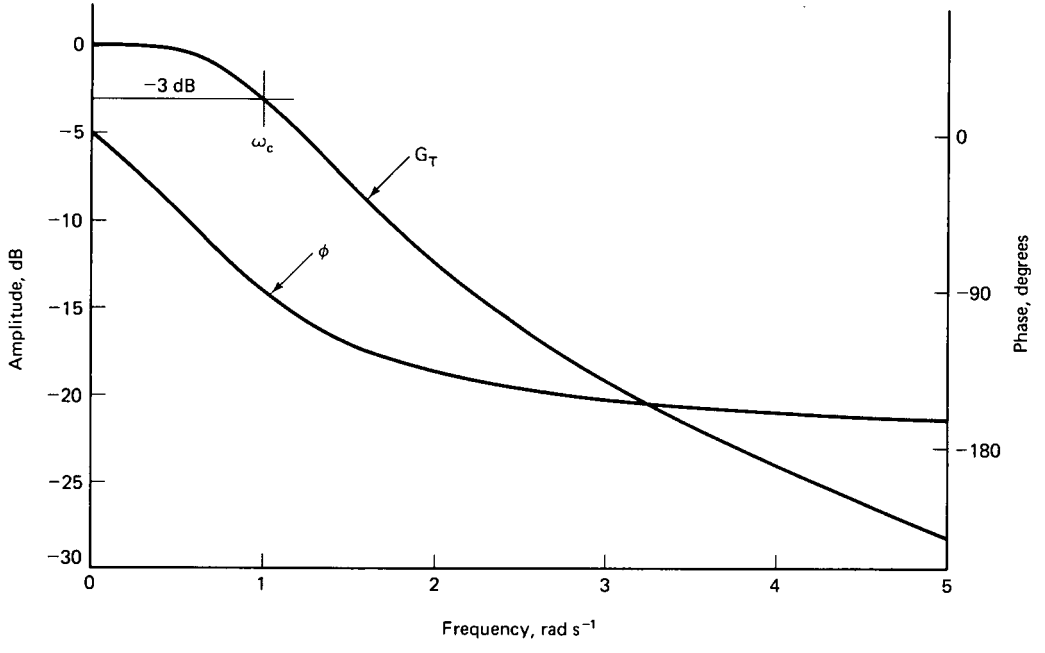

Figure 2.12 Frequency response, or transducer gain, G_t, of the two-pole low pass filter. Phase response is also shown.

Fig. 2.11. The phase with respect to the driving voltage generator is also presented. We have assumed a filter with equal terminations of 1 Ω and $C = \sqrt{2}$ F and $L = \sqrt{2}$ H.

This filter shows no attenuation near dc. However, $G_T = -3$ dB at a radian frequency of $\omega = 1$ rad s^{-1}. This is the cutoff frequency. Also, the phase is −90 degrees at the cutoff. The attenuation slope approaches 12 dB per octave and the phase nears −180 degrees at high frequencies.

The filter input impedance is also evaluated, shown in Fig. 2.11 as Z_f. The impedance is easily calculated in the frequency domain

$$Z_f(s) = sL + \frac{R_L}{1 + sCR_L} = \frac{(R_L LC)s^2 + sL + R_L}{1 + sCR_L} \tag{2.4-8}$$

The input impedance, like the transfer function, $H(s)$, is a ratio of polynomials. It has two zeros and one pole, which are evaluated using methods already presented.

The input impedance, $Z_f(j\omega)$ is calculated by substitution of $j\omega$ for s in Eq. 2.4-8. The results are plotted in Fig. 2.13 showing both the resistive and reactive portions. The imaginary part of the impedance is positive. This represents an inductive input. This is intuitively reasonable—at high frequencies the capacitor at the output of the filter tends to behave as a short circuit, leaving the inductor to dominate.

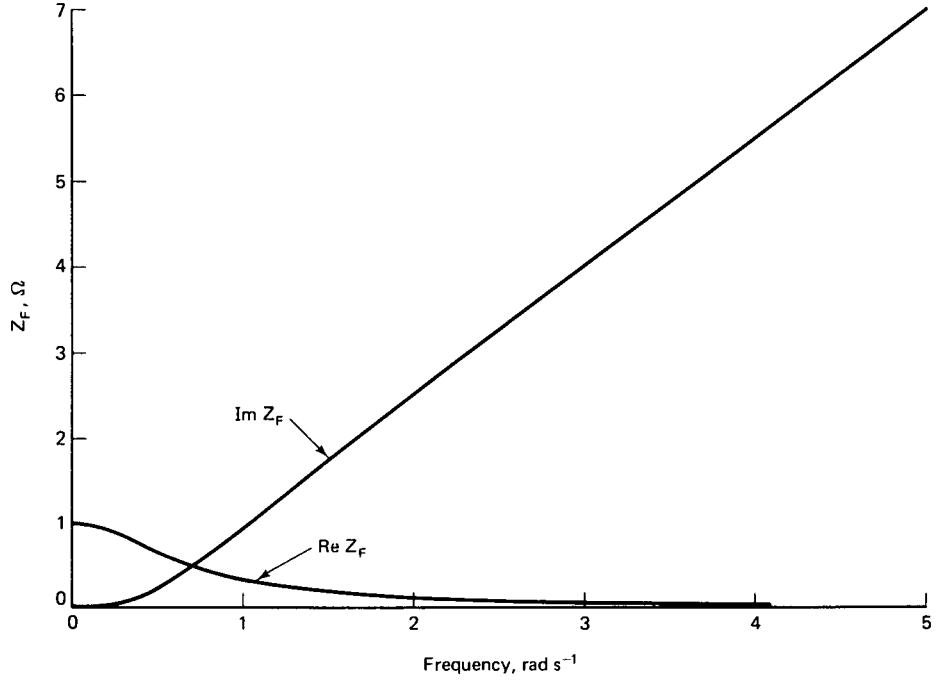

Figure 2.13 Input resistance and reactance for the two-pole, doubly terminated low poss filter.

The resistive portion of Z_f is 1 Ω and there is no reactance at dc and frequencies well below the cutoff. Maximum power is transferred and the attenuation is zero. The impedance changes when the frequency increases. Not only does the resistive portion tend toward zero, but the reactive part increases. This is characteristic of all *LC* filters. The filtering action is a result of mismatch between the source or load and the filter.

2.5 THE LADDER METHOD

The previous filter examples have been simple. They have contained at most two poles, representing two reactive components. Each time a reactive component is added, the degree of the polynomials describing the filter increases accordingly. Modern communications circuitry often requires filters with a dozen or more reactive components. The polynomials can, of course, be factored. However, the degree of algebraic cleverness required of the designer is at least commensurate with the degree of the polynomial. Other methods are required for the rest of us.

Our interest is not confined to the filter transfer function. We are also interested in the immittances (impedances or admittances) associated with the terminals of the filter. The filter must be properly terminated to function properly. Amplifiers at each end must be designed so that they not only function properly with the impedances presented at frequencies in the passband, but tolerate the impedances seen in the stopband.

A method is presented in this section that is especially suited to filters built in a ladder configuration. A ladder structure is one built from combinations of shunt and series elements. Some of the more complicated structures, such as the lattice, are not allowed. Fortunately, the ladder filter is a large category—nearly all of the typical filters in routine use are of this type. The method presented will not only evaluate the transfer function, but will provide impedance data. The method will be illustrated through the study of a third order low pass filter.

The first variation of the ladder method is sometimes termed the "tack hammer" approach. Any practical filter has a transfer function. It may not be known, but we can still write equations of a generalized form. A transfer function in the frequency domain, *H(s)*, has a corresponding steady state response, $H(j\omega)$. The ac output voltage at a given frequency is related to the input voltage by

$$V_{out} = H(j\omega)V_{in} \tag{2.5-1}$$

Solving for the input voltage yields

$$V_{in} = V_{out}H(j\omega)^{-1} \tag{2.5-2}$$

This suggests a method for filter analysis.

Figure 2.14 shows a third order low pass filter. We would speculate from the

intuition gained in previous examples that this filter would have no finite zeros and three poles in the transfer function, $H(s)$.

Two critical nodes, x and y, are labeled in Fig. 2.14. Assume that the output voltage across the load resistor, R_L, is 1 V. Knowing this, the voltage across the capacitor, C_3, is also known. Hence, the current out of node x is known. Specifically, the total current out of the node is the voltage times the admittance looking into the node from the left, or $I = G_L + j\omega C_3$. Arrows representing the direction of assumed current flow are included in the diagram.

The current out of node x equals that flowing in. Hence, the current flowing into the node, which is that flowing through the inductor, is also known. The voltage drop across the inductor is calculated from this. The voltage at node y is evaluated as $V_y = 1 + Y_x j\omega L_2$ where $Y_x = G_L + j\omega C_3$. Now that the voltage at node y is known, the current in C_1 is also specified. This defines the total current into node y from the generator.

The procedure is continued until the voltage at the generator is known. Note that the calculations all involve vectors, for the impedances and admittances are all complex. The transfer function is found from calculated input voltage, $H(j\omega) = V_{in}^{-1}$.

In addition, once the current into node y and the voltage at that node are calculated, the input immittance is defined.

This method is easily extended to an arbitrarily long ladder. It is only necessary to attack each node, one at a time in tack hammer fashion, until the filter is analyzed.

The tack hammer version of the ladder filter analysis involves the calculation of numerous immittances. Study suggests a slightly modified method, equivalent to the original, but with the virtue of being perhaps somewhat more ordered. Both are easily programmed with a handheld calculator.

Consider the vertical lines in Fig. 2.14. These are labeled with the letters "a" through "e" and represent different "planes" in the ladder filter. A different plane occurs whenever an additional component is added to the circuit. From each plane, an immittance (Z or Y) is well defined looking to the right toward the output termination.

The admittance is G_L at plane "a." Y_b, the admittance looking into plane "b," is $Y_a + j\omega C_3$. Knowing the admittance at plane "b," the corresponding impedance is calculated, the reciprocal of the admittance. When the admittance is complex, the conversion is performed by transforming from polar to rectangular coordinates.

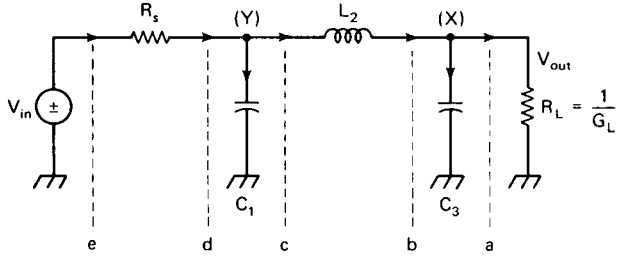

Figure 2.14 A three-pole low pass filter used to illustrate the ladder method of analysis.

The magnitude is replaced with its reciprocal and the sign of the angle is changed. The result is then converted back to rectangular coordinates.

The impedance looking to the right into plane "c" is that at plane "b" plus the inductive reactance of L_2. The result is then converted to an admittance and the admittance of C_1 is added. Another conversion results in Z_d. Finally, Z_e is obtained by addition of the source resistor. Y_e results from a final conversion.

The power of this calculation becomes evident with additional algebra. This is based upon having calculated all of the impedances or admittances at each plane in the filter. First, a value for V_{in} is specified. Typically, this will be 2 V, for we are interested ultimately in evaluation of filter transducer gain. The input current is now known, $I_e = V_{\text{in}} Y_e$. But this is also the current into plane "d." Knowing the current, the voltage at plane "d" is calculated. The procedure is repeated as needed. The method is summarized in the following set of equations

$$\begin{aligned} I_e &= V_{\text{in}} Y_e \\ I_d &= I_e \\ V_d &= I_e Z_d \\ I_c &= V_d Y_c \\ V_b &= I_c Z_b \end{aligned} \tag{2.5-3}$$

But V_b is the output voltage, V_{out}.

Examination of the family of equations, Eqs. 2.5-3, shows that each contains a current or a voltage on the right-hand side. However, that parameter is defined in the next equation above. A continued substitution will eventually terminate at the input voltage which was defined. The result is

$$V_{\text{out}} = Z_b Y_c Z_d Y_e V_{\text{in}} \tag{2.5-4}$$

This method appears formidable. It would be if it were done with a slide rule or with a very simple handheld calculator. However, modern programmable calculators make it a relatively simple task.

Each stage in the calculation involves the conversion of an impedance to an admittance, or the opposite. It is necessary to perform a rectangular to polar conversion at each step. Upon taking the reciprocal of the magnitude and changing the sign of the angle, the desired result is available, the needed new immittance. The magnitude can be multiplied into a storage register and the angle summed into another. The polar result is converted back into a rectangular format. This is needed to add the next series impedance or shunt admittance. The transfer function is generated "for free" during the calculation of the input immittance seen from the driving generator.

An order is present in Eq. 2.5-4 that may not be immediately apparent. The product of immittances is alternating in type. That is, the products are an impedance

followed by an admittance followed by an impedance, etc. Also, admittances correspond to planes looking into series elements while impedances correspond to filter planes looking into parallel elements. This allows a program to be written quickly.

2.6 LOSSES IN REACTIVE COMPONENTS AND QUALITY FACTOR

The parameter Q was introduced in a preceding section dealing with the series tuned circuit. No explanation was presented other than observing that the bandwidth of the circuit decreased as Q increased. This section will present a more formal definition and rationale for the parameter and will show how it is used in network analysis.

We have assumed in our studies that components are ideal. This implies that they show no loss. This is, of course, not realistic. It is only a model that serves for analysis. Real components do have loss.

There are numerous mechanisms that will produce loss in capacitors and inductors. Dielectric heating and surface resistance on the conducting elements often introduce loss in capacitors. Inductors show loss from motion of magnetic core material and from wire resistance. The physics surrounding these phenomena is interesting and of vital concern to rf designers, especially those working at microwave frequencies.

The inherent loss mechanisms resulting from component imperfections are usually beyond the control of the designer. They must be taken into account during analysis though. Sometimes loss is purposefully introduced into a circuit. The most common example is the termination that is found with any practical network. If there was no termination, it would not be possible to extract energy from the network and the circuit would have no purpose. All of these losses are represented with the parameter Q, which stands for the quality factor.

Formally, the Q of a circuit is defined as 2π times the energy stored in the circuit divided by the energy lost per cycle of oscillation. The Q concept is usually applied to a resonant or tuned circuit, which is often called a resonator. When applied to a single component the Q is that which would result from resonating the component at the frequency of interest with an ideal lossless reactance of the opposite type. That is, the Q of an inductor would be the Q of a tuned circuit using that inductor with a lossless capacitor.

It may be shown that the Q of an inductor can be modeled by a series resistor (6). The resistor value is

$$R_s = \frac{\omega L}{Q} \tag{2.6-1}$$

This resistor represents either the internal losses of the nonideal inductor or the external loss associated with a load combined with internal losses. If the Q value represents only the internal losses, the nonideal nature of the component, the Q is termed the "unloaded Q" and is signified by a subscript, Q_u. It is termed Q_L for "loaded Q" if the Q value represents external loads as well as the internal losses.

The higher the Q, the smaller the series resistance and hence the smaller the loss. This is seen from the definition, Eq. 2.6-1.

We have seen in our study of networks that impedance and admittance are used interchangeably. Admittance is more convenient than impedance when evaluating a shunt component. Similarly, Q may be represented by a parallel instead of a series resistance.

The impedance of a real inductor, as modeled by Q, is $j\omega L + R_s$. The admittance is then

$$Y = \frac{1}{j\omega L + R_s} \tag{2.6-2}$$

Multiplying the top and bottom by the complex conjugate of the denominator and inserting Eq. 2.6-1 for R_s yields

$$Y = \frac{(\omega L/Q) - j\omega L}{\frac{\omega^2 L^2}{Q^2} + \omega^2 L^2} \tag{2.6-3}$$

The admittance is of the form $G + jB$ where G is a conductance, $G = 1/R_p$, and B is a susceptance, $B = 1/X_p$. Separating Eq. 2.6-3 into real and imaginary parts yields, upon multiplication by Q^2

$$Y = \frac{1}{R_p} - j\frac{1}{X_p} = \frac{Q\omega L}{\omega^2 L^2(1 + Q^2)} - j\frac{\omega L Q^2}{\omega^2 L^2(1 + Q^2)} \tag{2.6-4}$$

For large value of Q, $(1 + Q^2) \simeq Q^2$. Hence

$$R_p \simeq Q\omega L \qquad X_p \simeq \omega L \tag{2.6-5}$$

Both forms of modeling are used almost interchangeably in practice. The choice is usually one of convenience. The difference is only significant for Q values of less than 10.

Practical inductors show a wide range of Q_u values. They are always a function of frequency. Q increases with frequency, usually in proportion to the square root of the frequency for a given fixed size air core inductor. Inductors wound on a powdered iron core typically have a peak in Q_u as frequency is changed. The best inductors are thus built with a core picked especially for the frequency range of interest. The highest Q_u values are usually obtained with toroidal cores for the hf region. Larger Q_u values result from air cores, but the physical size is often unreasonable. A typical high Q inductor in the hf range would have $Q_u = 250$ or higher.

If large wire is used at vhf, air core inductors become practical. It is easily possible to achieve Q_u greater than 400 if large wire is used. This is best realized if

the inductor is shielded, owing to radiation losses. The Q of the components should be measured or obtained from tables provided by manufacturers of powdered iron cores if careful work is to be done (7).

Capacitors also suffer from losses which may be represented by a Q_u. Assume a capacitor has a loss that is modeled by a parallel resistance, R_p. If this capacitor was placed in parallel with a perfect, lossless inductor, the resonator would have an unloaded Q_u equal to that of the capacitor. If Q_u was associated with the inductor, R_p would be $Q_u\omega L$. The inductive susceptance equals that of the capacitor in the resonant circuit. Hence

$$R_p = \frac{Q_u}{\omega C} \tag{2.6-6}$$

Following the same arguments as were used with the inductor, the Q_u value of a capacitor may be related to a series resistance, R_s, by

$$R_s = \frac{1}{Q_u\omega C} \tag{2.6-7}$$

As was the case with the inductor, Eqs. 2.6-6 and 2.6-7 are not exactly related to each other. The two depend upon high Q_u values. We will use $R_p = Q_u\omega L = Q_u/\omega C$ as a formal relationship in most of our work.

Most capacitors used in tuned circuits have a very high Q_u in the hf region. Values well over 1000 are typical. Hence, it is valid for most applications to assume that parallel capacitors are lossless and that the loss of a circuit is related to the inductor.

This ideal behavior is not always true. At vhf and higher, capacitors often exhibit Q values that are low enough that they must be taken into account in analysis. This is true even in the hf spectrum with some capacitors. An example of a lossy capacitor is the varactor diode often used as a voltage controlled variable capacitor. The manufacturers of such diodes usually specify the Q_u at a stated frequency with the understanding that Q_u will decrease linearly with increasing frequency. A better model is that of an ideal diode with a frequency independent series resistance.

Consider the parallel tuned resonator of Fig. 2.15 as an example of the effect of Q in a tuned system. Assume that the source equals the load resistance. Using methods developed earlier, the transfer function is

$$H(s) = \frac{sL/R}{s^2LC + 1 + 2sL/R} \tag{2.6-8}$$

We find that $H(j\omega) = \frac{1}{2}$ at $\omega^2 = 1/LC$. Hence, all of the power available from the voltage generator and source resistance is being delivered to the load resistor. The resonator is transparent at this frequency, that of resonance.

The transfer function may be compared with that of the series tuned circuit,

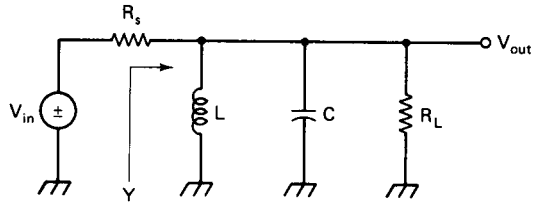

Figure 2.15 A parallel tuned circuit, doubly terminated.

Eq. 2.3-3. Some manipulation then shows that the Q equals half that of the series tuned circuit. However, the series tuned circuit studied contained only one resistor while the parallel one of Fig. 2.15 has two. The circuit Q is thus given by $Q_L = R_p/\omega L$ where R_p is now the parallel combination of the source and load resistors. Note that the same form of transfer function describes both the series and the parallel tuned circuit.

Assume now that the components in the filter of Fig. 2.15 are not ideal, but have a loss described by measurable Q_u values. The equivalent parallel resistance associated with the inductor is $R_{pL} = Q_{uL}\omega L$ while the loss in the capacitor is $R_{pC} = Q_{uC}/\omega C$. But $L = 1/\omega C$. The equivalent loss resistance is the parallel combination of the two. The final result is the equivalent Q_u

$$Q_{\text{net}} = (Q_{uL}^{-1} + Q_{uC}^{-1})^{-1} \tag{2.6-9}$$

This equation is quite general. When a number of lossy reactances are connected in parallel or in series, the equivalent Q is obtained in the same way that the equivalent resistance of parallel resistors is obtained.

Assume that the Q_u value of the capacitor is arbitrarily high. The Q_u of the tuned circuit is then that of the inductor alone, resulting in $R_p = Q_u\omega L$. The effects of the reactive components disappear at resonance, leaving the equivalent circuit shown in Fig. 2.16. The transducer gain of this network will be evaluated. We assume that $R_s = R_L = R$ and the voltage generator has an amplitude of 2 V. The output voltage is written from inspection. Algebraic reduction produces the result

$$V_{\text{out}} = \frac{2\left(\dfrac{R_pR}{R+R_p}\right)}{R+\dfrac{R_pR}{R+R_p}} = \frac{1}{1+R/2R_p} \tag{2.6-10}$$

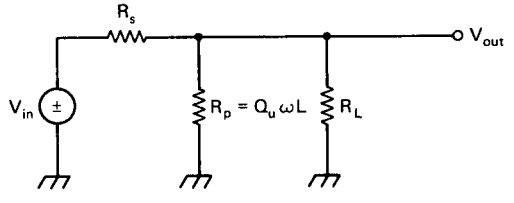

Figure 2.16 The equivalent of the parallel tuned circuit at resonance. R_p is the resistance representing the losses in the resonator.

The unloaded Q is $Q_u = R_p/\omega L$ while the loaded Q is $Q_L = R_e/\omega L$ where R_e is the equivalent resistance loading the inductor. R_e is the parallel combination of the load, the source, and R_p. Hence

$$R_e = \frac{R_p R}{2R_p + R} \tag{2.6-11}$$

for the case of equal load and source resistances.

Consider the ratio of Q_L/Q_u

$$\frac{Q_L}{Q_u} = \frac{R_e}{R_p} = \frac{R}{2R_p + R} \tag{2.6-12}$$

This simplifies to the relationship

$$\frac{R}{2R_p} = \frac{Q_L}{Q_u - 1} \tag{2.6-13}$$

which is then inserted into Eq. 2.6-10 to produce

$$V_{\text{out}} = \left(1 - \frac{Q_L}{Q_u}\right) \tag{2.6-14}$$

Because the source and load resistances are equal, the insertion loss of the filter of Fig. 2.15 is the negative of the transducer gain, or

$$\text{Insertion loss (IL)} = -20 \log (1 - Q_L/Q_u) \text{ db} \tag{2.6-15}$$

This filter is a doubly terminated single resonator.

The bandwidth of the single resonator, terminated or not, is analytically related to the Q. Recalling that the bandwidth is defined as the frequency where the output power is down by half, or 3 dB, bandwidth is related to center frequency and Q by

$$Q = f_0/\text{BW} \tag{2.6-16}$$

where F_0 and BW are both measured in the same units.

This is well illustrated by an example. Assume a resonator has a center frequency of 100 MHz and $Q_u = 400$. The unloaded bandwidth is 100/400 = 0.25 MHz (Q is a dimensionless number). A bandwidth of 1 MHz is measured if the resonator is then placed between an equal source and load. The loaded Q is then $Q_L = 100/1 = 100$. The insertion loss from Eq. 2.6-15 is 2.5 dB.

Examination of the equations reveals a method for measuring the Q of a resonator. Note that as the loaded Q of a filter approaches the unloaded value, the insertion

loss becomes very large. If a resonator is terminated equally by both the generator and load and the values are adjusted so that the insertion loss is very large, the measured 3-dB bandwidth will produce a loaded Q according to Eq. 2.6-16. Measuring the insertion loss will allow calculation of Q_L/Q_u. The loaded Q is very close to Q_u if the insertion loss is high enough, typically 30 to 40 dB.

Q has been related to a second order network in our discussion. That is, Q is a parameter of a network containing two reactive elements, described by a transfer function of second order. Sometimes a parameter Q appears in design equations for third or even fourth order networks. The meaning for this Q is only loosely related to the Q parameter we have been discussing. The actual energy storage in the network and the related bandwidth properties are sometimes completely unrelated to Q.

2.7 THE ALL-POLE LOW PASS FILTER

Previous sections have presented background information and analysis methods. Now, the problem of filter design is finally approached. The type of filter considered in this section is shown in Fig. 2.17. It contains only series inductors and shunt capacitors. The filter is a ladder configuration and may be analyzed using the ladder method presented earlier.

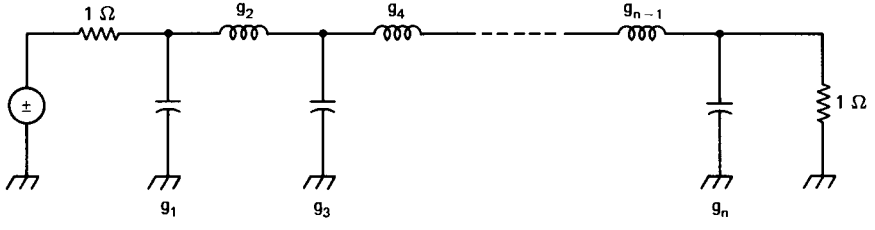

Figure 2.17 An nth order low pass filter. The text has equations for evaluating the component values and the location of the poles.

We find that the transfer function, $H(s)$, of the filter of Fig. 2.17 contains no finite zeros. The transfer function is the reciprocal of a simple polynomial in the variable s. As such, the filter is described completely by factoring of the denominator polynomial to extract the location of the complex poles. This filter, an *all-pole* type, represents many of the practical low pass filters used in routine rf design.

Most design work with all filters is done with low pass prototypes like that of Fig. 2.17 where the source and load resistance are 1 Ω and the cutoff frequency is 1 rad. This has a number of consequences. First, analysis is simplified. Second, the normalized filters are in a form that may be easily scaled to other terminations and cutoff frequencies. The final rationale is somewhat less obvious, though. At a frequency of 1 rad s^{-1}, a 1-H inductor and a 1-F capacitor have the same immittance, 1 Ω or 1 Siemen (S). This duality allows us to treat them more easily than we could if another frequency of normalization were chosen. One consequence is that one form of filter may be transformed into another with no change in numerical values.

This duality is illustrated by the two filters in Fig. 2.18. One has two capacitors of 1 F and an inductor of 2 H. The other has two inductors of 1 H each and a single capacitor of 2 F. Both of these filters are identical. The cutoff frequency (−3 dB) is 1 rad s^{-1} and the transfer functions, *H(s)*, are identical. Only one set of normalized parameters is required for tabulation of normalized filter components. These are usually given by g_k as shown in the component labeling of Fig. 2.17.

The defining polynomial has a degree that is numerically identical to the number of reactive components in the prototype filter. The filters of Fig. 2.18 are third order filters with the highest power of *s* in *H(s)* being 3. The filter g_k values are chosen for a cutoff of 1 rad s^{-1}. However, there are no other restrictions. An infinite number of component values are still allowed.

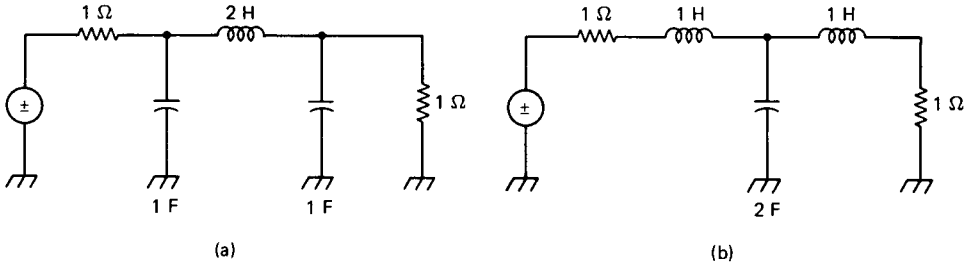

Figure 2.18 Two different, but equivalent versions of the three-pole normalized Butterworth low pass filter.

The chore of picking useful components is a complicated one and is the essence of much of the subject of filter synthesis. Approximation methods are usually applied. An ideal filter serves as a starting point. Then, an attempt is made at choosing filter polynomials which approximate one characteristic or another of the ideal filter. The term "ideal" is itself something of a puzzle. A filter that has a perfect "brick wall" shape in the frequency domain, such as the low pass filter of Fig. 2.8a, may have a horrible step response.

The nature of the approximations used in synthesis is covered well by many writers and will not be dealt with here. The curious reader should refer to the text by Blinchikoff and Zverev.

This section will present two popular and practical polynomial types and the corresponding filters, the Butterworth and Chebyshev. The Butterworth filter is optimized near the lowest frequencies and is often called a maximally flat response. It has reasonable time domain behavior although not as ideal as some other types.

The Chebyshev filter is optimized for frequency domain response. It has excellent differentiation between the passband response and that of the stopband. The price for these virtues is some ripple, or variation, in attenuation within the passband and poor time domain response.

The frequency response of the normalized Butterworth filter is

$$H(j\omega) = \frac{1}{(1 + \omega^{2n})^{1/2}} \tag{2.7-1}$$

where ω is the angular frequency and n is the degree of the polynomial. Using this frequency response, the parameter values, the location of the complex poles, and the frequency domain transfer function may all be derived. The pole locations in the s plane are given by

$$\sigma_k = -\sin(2k-1)\frac{\pi}{2n} \qquad \omega_k = \cos(2k-1)\frac{\pi}{2n} \qquad k = 1, 2, 3, \ldots, n \tag{2.7-2}$$

where σ_k is the real part and ω_k is the complex part of the kth pole. The pole locations may be combined with s to form the factored form of $H(s)$. Multiplication will produce the usual form. The transfer functions for $n = 2$ and $n = 3$ are

$$H(s) = \frac{1}{s^2 + 1.414s + 1} \qquad n = 2$$
$$H(s) = \frac{1}{s^3 + 2s^2 + 2s + 1} \qquad n = 3 \tag{2.7-3}$$

For larger values of n, the polynomials become more complex.

Noting the pole locations, Eqs. 2.7-2, we see that the real and complex parts are described by a sine and a cosine function with the same argument. Hence, the poles of the Butterworth low pass filter lie on a circle in the s plane.

The component values of the normalized Butterworth low pass are given by

$$g_k = 2\sin(2k-1)\frac{\pi}{2n} \qquad k = 1, 2, 3, \ldots, n \tag{2.7-4}$$

for the case where the source and load resistances are 1 Ω. As it turns out, this restriction is not a firm one. The end terminations need not be equal with proper renormalization. The reader should refer to the literature for details (8).

The function for component values, Eq. 2.7-4, is an especially simple relationship. Consider $n = 3$. Substitution then yields $g_1 = 1$, $g_2 = 2$, and $g_3 = 1$. The resulting filters are those of Fig. 2.18.

The analytical representation of the Chebyshev filters is considerably more complex than the Butterworth. Where the Butterworth filter was described by circular functions, the Chebyshev is dominated by hyberbolic functions. These are somewhat more complicated, but may be manipulated easily with a programmable handheld calculator. The analog to the Euler identities can be used:

$$\sinh x = \frac{e^x - e^{-x}}{2} \qquad \cosh x = \frac{e^x + e^{-x}}{2} \tag{2.7-5}$$

The frequency response of the Chebyshev low pass filter is given by

$$H(j\omega) = \frac{1}{[1 + \epsilon^2 C_n^2(\omega)]^{1/2}} \tag{2.7-6}$$

where $C_n(\omega)$ are the Chebyshev polynomials defined by

$$\begin{aligned} C_n(\omega) &= \cos(n \cos^{-1}\omega) \qquad \omega < 1 \\ C_n(\omega) &= \cosh(n \cosh^{-1}\omega) \qquad \omega > 1 \end{aligned} \tag{2.7-7}$$

The parameter ϵ is the ripple in the passband and is given by

$$\epsilon = (10^{0.1A} - 1)^{1/2} \tag{2.7-8}$$

where A is the depth of the ripple in dB.

Figure 2.19 will shed additional light on the nature of the Chebyshev filter. The figure shows the $H(j\omega)$ plot for a filter with $n = 5$ and $A = 1.5$ dB. The frequency response of the filter oscillates by a peak-to-peak value of 1.5 dB throughout

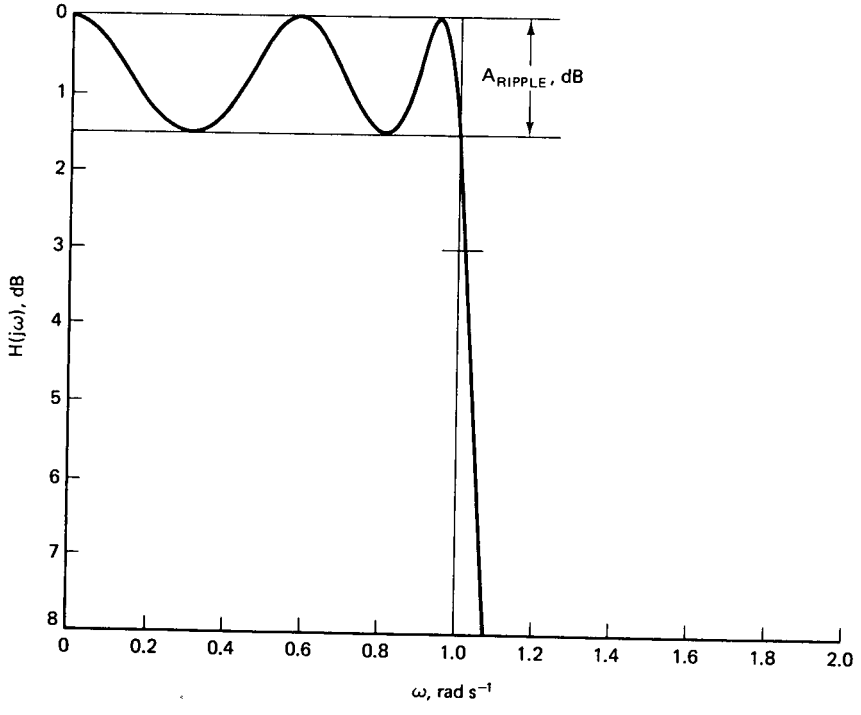

Figure 2.19 Frequency response of a five-pole low pass filter of the Chebyshev type. The passband ripple is $A = 1.5$ dB. The attenuation equals the ripple at the cutoff frequency of 1 rad s^{-1}. Note that the number of half cycles of passband ripple equals the order of the filter.

the passband. One other feature is apparent in Fig. 2.19. The response at $\omega = 1$ rad s^{-1} is equal to the value of A, the ripple, and is not -3 dB as is usually the case. The frequency where the response is down by 3 dB is given by

$$\omega_{3dB} = \cosh\left(\frac{1}{n}\cosh^{-1}\frac{1}{\epsilon}\right) \tag{2.7-9}$$

for $A < 3$ dB.

The number of poles in a Chebyshev filter is equal to the number of half cycles of oscillation in the ripple passband response. N was 5 for the filter used for the curve of Fig. 2.19. Hence, at dc, the response was zero dB, or unity, for evaluation of Eq. 2.7-6. This cannot be true for n an even number and preserve the Chebyshev response of Eq. 2.7-6 unless the source and load reactances are unequal. If the load is kept at 1 Ω, the required source resistance to preserve the desired filter shape is given by

$$R_s = \begin{cases} 1, & n \text{ odd} \\ \tanh^2\left(\dfrac{B_0}{4}\right), & n \text{ even} \end{cases} \tag{2.7-10}$$

where the parameter B_0 is defined below.

The equations for the component values, g_k, of the Chebyshev low pass filter are standard and are presented in many texts. They are rarely presented in a closed form. Instead, several equations of related parameters are given that are then used to calculate the g_k values. A modified version of these equations is presented below where the hyperbolic functions have been replaced by their exponential equivalents. This facilitates evaluation with a handheld calculator.

The set of equations appears formidable. It is not. A program is easily written for the handheld calculator to evaluate the functions. The following set of equations also contains the adaptations of Eqs. 2.7-9 and 2.7-10 in an exponential form

$$d = \frac{A}{8.68589} \tag{2.7-11}$$

where A is the passband ripple in dB.

$$B = \frac{1}{2n}\ln\left[\frac{e^d + 1}{e^d - 1}\right] \tag{2.7-12}$$

$$B_0 = 2nB \tag{2.7-13}$$

$$N = \tfrac{1}{2}(e^B - e^{-B}) \tag{2.7-14}$$

$$a_k = \sin\left[\frac{(2k-1)\pi}{2n}\right] \qquad k = 1, 2, \ldots, n \tag{2.7-15}$$

$$b_k = N^2 + \sin^2\left(\frac{k\pi}{n}\right) \qquad k = 1, 2, 3, \ldots, n \tag{2.7-16}$$

The g_k values are calculated using these parameters

$$g_1 = \frac{2a_1}{N} \tag{2.7-17}$$

$$g_k = \frac{4a_{k-1}a_k}{b_{k-1}g_{k-1}} \tag{2.7-18}$$

The 3-dB down frequency is evaluated using

$$\omega_{3\text{dB}} = \tfrac{1}{2}(e^{Y} + e^{-Y}) \tag{2.7-19}$$

where Y is given by

$$Y = \frac{1}{n}\ln\left[\frac{1}{\epsilon} + \left(\frac{1}{\epsilon^2} - 1\right)^{1/2}\right] \tag{2.7-20}$$

for $A <$ 3-dB ripple. The source required for proper termination to produce the Chebyshev response in an even order filter is

$$R_s = \left[\frac{e^{2x} - 1}{e^{2x} + 1}\right]^2 \tag{2.7-21}$$

where

$$x = \frac{B_0}{4} \tag{2.7-22}$$

The parameters a_1, b_1, and g_1 are calculated. Then these values are used, along with a_2 and b_2, to evaluate g_2. This continues. The evaluation of the kth component depends upon earlier calculations associated with $k - 1$.

Table 2.1 is a tabulation of some results of these equations. The g_k values are presented for filters from order 2 through 5. The cases shown are for the Butterworth filter, shown as $A = 0$, and Chebyshev filters with passband ripple of $A = 0.1$, 0.25, 0.5, 0.75, 1.0, and 1.5 dB. The frequencies where the attenuation is -3 dB are also shown as well as the source resistances needed for achieving the Chebyshev response.

Table 2.1 g_k Values for Chebyshev and Butterworth ($A = 0$) Low Pass Filters. (Normalized to $R_L = 1\ \Omega$ and a ripple bandwidth of 1 rad s^{-1})

A, dB	n	g_1	g_2	g_3	g_4	g_5	R_s^{-1}	ω, −3 dB
0	3	1.000	2.000	1.000	—	—	1.000	1.000
	4	0.7654	1.8478	1.8478	0.7654	—	1.000	1.000
	5	0.6180	1.618	2.000	1.6180	0.618	1.000	1.000
0.1	2	0.8430	0.6220	—	—	—	0.7378	1.9432
	3	1.0316	1.1474	1.0316	—	—	1.000	1.3890
	4	1.1088	1.3062	1.7704	0.8181	—	0.7378	1.2131
	5	1.1468	1.3712	1.9750	1.3712	1.1468	1.000	1.1347
0.25	2	1.1132	0.6873	—	—	—	0.6174	1.5981
	3	1.3034	1.1463	1.3034	—	—	1.000	1.2529
	4	1.3782	1.2693	2.0558	0.8510	—	0.6174	1.1398
	5	1.4144	1.3180	2.2414	1.3180	1.4144	1.000	1.0887
0.5	2	1.4029	0.7071	—	—	—	0.504	1.3897
	3	1.5963	1.0967	1.5963	—	—	1.000	1.1675
	4	1.6703	1.1926	2.3661	0.8419	—	0.504	1.0931
	5	1.7058	1.2296	2.5408	1.2296	1.7058	1.000	1.0593
0.75	2	1.6271	0.7002	—	—	—	0.4304	1.2852
	3	1.8243	1.0436	1.8243	—	—	1.000	1.1236
	4	1.8988	1.1243	2.6124	0.8172	—	0.4304	1.0689
	5	1.9343	1.1551	2.7833	1.1551	1.9343	1.000	1.0439
1.00	2	1.8219	0.6850	—	—	—	0.3760	1.2176
	3	2.0236	0.9941	2.0236	—	—	1.000	1.0949
	4	2.0991	1.0644	2.8311	0.7892	—	0.3760	1.0530
	5	2.1349	1.0911	3.0009	1.0911	2.1349	1.000	1.0338
1.50	2	2.1688	0.6470	—	—	—	0.2983	1.1307
	3	2.3803	0.9069	2.3803	—	—	1.000	1.0574
	4	2.4586	0.9637	3.2300	0.7335	—	0.2983	1.0322
	5	2.4956	0.9850	3.4017	0.9850	2.4956	1.000	1.0205

Other characteristics of the Chebyshev filter are apparent from the table. Looking at the −3-dB frequencies, it is seen that the rate of attenuation increases both for increasing n and for increased passband ripple. If passband ripple is allowed, but as much stopband attenuation as possible is needed, the Chebyshev low pass filter with high ripple is called for. If the passband must be "clean" with a minimum of ripple, the Butterworth, or a low ripple Chebyshev, is the choice.

Evaluation of the 3-dB frequencies gives some indication of the rate of attenuation as the frequency moves from the passband to the stopband. However, it is less than analytical. Knowledge of the stopband characteristics is often of great importance in filter specification. As often as not, the desired goal is to provide a given level of attenuation at a specific frequency that is out of the passband of a filter. Table 2.2 presents this data.

Table 2.2 shows the attenuation values in the stopband for $\omega = 1, 2, 3, 4, 5, 6, 8$, and 10. All of the filters presented in Table 2.1 are considered. The data in the stopband attenuation table is extended to filters up to the seventh order.

Table 2.2 Attenuation values in dB for Butterworth and Chebyshev filters for orders from 2 to 7. $\omega = 1$ corresponds to the edge of the ripple band for Chebyshev filters and the 3-dB point for the Butterworth filter.

Table 2.2a Butterworth Filter

n	1	2	3	4	5	6	8	10
2	3.0	12.3	19.1	24.1	28.0	31.1	36.1	40.0
3	3.0	18.1	28.6	36.1	41.9	46.7	54.2	60.0
4	3.0	24.1	38.2	48.2	55.9	62.3	72.2	80.0
5	3.0	30.1	47.7	60.2	69.9	77.8	90.3	100.0
6	3.0	36.1	57.3	72.2	83.9	93.4	108.4	120.0
7	3.0	42.1	66.8	84.3	97.9	108.9	126.4	140.0

Table 2.2b 0.1-dB Chebyshev Filter

n	1	2	3	4	5	6	8	10
2	0.1	3.3	8.9	13.7	17.6	20.7	25.8	29.7
3	0.1	12.2	23.6	31.4	37.4	42.2	49.8	55.6
4	0.1	23.4	38.9	49.3	57.3	63.7	73.8	81.6
5	0.1	34.8	54.2	67.3	72.2	85.3	97.9	107.6
6	0.1	46.3	69.5	85.2	97.1	106.8	121.9	133.6
7	0.1	57.7	84.8	103.1	117.0	128.3	146.0	159.0

Table 2.2c 0.25-dB Chebyshev Filter

n	1	2	3	4	5	6	8	10
2	0.25	5.9	12.6	17.6	21.6	24.8	29.8	33.7
3	0.25	16.1	27.6	35.5	41.4	46.3	53.9	59.7
4	0.25	27.5	43.0	53.4	61.4	67.8	72.9	85.7
5	0.25	38.9	58.3	71.4	81.3	89.3	101.9	111.7
6	0.25	50.3	73.6	89.2	101.2	110.8	126.0	137.7
7	0.25	61.8	88.9	107.2	121.1	132.4	150.0	157.3

Table 2.2d 0.5-dB Chebyshev Filter

n	1	2	3	4	5	6	8	10
2	0.5	8.4	15.6	20.7	24.7	27.9	32.9	36.8
3	0.5	19.2	30.8	38.6	44.6	49.4	57.0	62.8
4	0.5	30.6	46.1	56.5	64.5	70.9	81.0	88.8
5	0.5	42.0	61.4	74.5	84.4	92.5	105.1	114.8
6	0.5	53.5	76.7	92.4	104.3	114.0	129.1	140.8
7	0.5	64.9	92.0	110.3	124.2	135.5	153.2	166.8

Table 2.2e 0.75-dB Chebyshev Filter

n	1	2	3	4	5	6	8	10
2	0.75	10.1	17.4	22.6	26.6	29.8	34.8	38.7
3	0.75	21.1	32.7	40.5	46.5	51.3	58.9	64.7
4	0.75	32.5	48.0	58.4	66.4	72.8	82.9	90.7
5	0.75	43.9	63.3	76.3	86.3	94.3	107.0	116.7
6	0.75	55.4	78.6	94.3	106.2	115.9	131.0	142.7
7	0.75	66.8	93.9	112.2	126.1	137.4	155.1	168.7

Table 2.2f 1.0-dB Chebyshev Filter

n	1	2	3	4	5	6	8	10
2	1.0	11.4	18.8	24.0	27.9	31.6	36.2	40.1
3	1.0	22.5	34.0	41.9	47.8	52.7	60.3	66.1
4	1.0	33.9	49.4	59.8	67.8	74.2	84.3	92.1
5	1.0	45.3	64.7	77.7	87.7	95.7	108.4	118.1
6	1.0	56.7	80.0	95.6	107.6	117.2	132.4	144.1
7	1.0	68.2	95.3	113.6	127.5	138.8	156.4	170.1

Table 2.2g 1.5-dB Chebyshev Filter

n	1	2	3	4	5	6	8	10
2	1.5	13.3	20.8	26.0	30.0	33.2	38.2	42.1
3	1.5	24.5	36.1	43.9	49.9	54.7	62.3	68.1
4	1.5	35.9	51.4	61.8	69.8	76.2	86.3	94.1
5	1.5	47.3	66.7	79.7	89.7	97.7	110.4	120.1
6	1.5	58.8	82.0	97.7	109.6	119.3	134.4	146.4
7	1.5	70.2	97.3	115.6	129.5	140.8	158.5	172.1

Care must be exercised in using the data in Table 2.2, for the standard Chebyshev equations have been used in evaluation. Hence, for a Chebyshev filter with a passband ripple of 0.25 dB, the attenuation at $\omega = 1$ will be 0.25 dB. Data on the −3-dB frequencies given in Table 2.1 will allow the data of Table 2.2 to be normalized to −3 dB as needed. Similar data are presented in graphical form by Zverev (9) where all information has been normalized to a 3-dB cutoff frequency.

Use of these tables is illustrated by an example. Assume a low pass filter is to be built with the specification that the stopband attenuation should be greater than 60 dB. The stopband, in this case, will be defined as frequencies greater than twice the edge of the ripple band. We find upon examining $\omega = 2$ that attenuations greater than 60 dB occur for the seventh order Chebyshev filters with a ripple of 0.25 dB or more.

The Butterworth filter has an advantage that is not apparent from the calculations. It has the virtue that it is generally insensitive to small changes in component

values. This is demonstrated by differentiating the salient equations with respect to component value. The Chebyshev response, however, is much more dependent upon careful component selection.

The symmetry of the filters is interesting. The Butterworth filters are always symmetrical with respect to component value. That is, equal g_k values appear about a centerline drawn through the filter. The odd ordered Chebyshev filters are also symmetrical. This is not true for the even order Chebyshev prototypes though.

The location of the poles of the Chebyshev filter are given as

$$\sigma_k = \sinh N \sin(2k-1)\frac{\pi}{2n}$$
$$\omega_k = \cosh N \cos(2k-1)\frac{\pi}{2n} \tag{2.7-23}$$

where N is given by

$$N = \frac{1}{n}\sinh^{-1}\frac{1}{\epsilon} \tag{2.7-24}$$

It may be shown that the poles of the Chebyshev filter lie on an ellipse. They are, of course, in the left half of the s plane. The ellipse is inside the circle of the Butterworth filter. This is significant. It indicates that the real part of the poles of the Chebyshev filter have a smaller magnitude than the Butterworth does. Hence, damping is not as great—the poles have a higher Q than do those of an equal ordered Butterworth filter. This is reflected in the time domain responses. The Chebyshev filter shows more overshoot in both the impulse and step responses than does the Butterworth. For this reason, the Chebyshev is not recommended for applications where very high transition rates are encountered, such as pulses.

The Butterworth filter has a somewhat improved response to an impulse and a step than the Chebyshev does. However, it is still not optimum. Other polynomials are suggested for improved time domain response. These include the Bessel, the Gaussian, and the minimum phase ripple filters. These are covered in detail in the work of Zverev (9).

2.8 FILTER DENORMALIZATION, PRACTICAL LOW PASS, HIGH PASS, AND BANDPASS STRUCTURES

The previous section showed how normalized components were calculated for low pass filters. It is rare indeed when filters are built for a cutoff frequency near 1 rad s^{-1} and a 1-Ω termination. Impedances are usually higher and cutoff frequencies are arbitrary. The equations for denormalization of the previous filters will be presented in this section.

A low pass filter may begin with the first component being either a capacitor or an inductor. The next component in the ladder must, however, be of the opposite type. Each additional part must be opposite from the previous.

Intuition will generally prevail in the denormalization process. If a termination impedance higher than 1 Ω is desired, the reactances are multiplied accordingly. The reactances are then scaled so that they have the same value at the new desired cutoff frequency, ω_c. The stopband attenuation values presented in Table 2.2 will scale with ω replaced by the ratio of the actual cutoff to the frequency where a given value of attenuation is observed.

The high pass filter is the dual of the low pass. Series inductors are replaced with series capacitors while shunt capacitors are replaced by inductors. The reactances are the same at the normalized cutoff of 1 rad s^{-1}.

The components for a low pass filter based upon the normalized results, Table 2.1, are

$$C_k = \frac{g_k}{R_0 \omega_c} \tag{2.8-1}$$

and

$$L_k = \frac{g_k R_0}{\omega_c} \tag{2.8-2}$$

The high pass filter is described by the following denormalization of the normalized low pass tables

$$C_k = \frac{1}{g_k R_0 \omega_c} \tag{2.8-3}$$

and

$$L_k = \frac{R_0}{\omega_c g_k} \tag{2.8-4}$$

In all of the equations above, $\omega_c = 2\pi f_c$ where f_c is the cutoff frequency in hertz (Hz), and R_0 is the termination in ohms.

Assume that low pass and high pass filters with a Butterworth response are to be built with a cutoff frequency of 5 MHz and terminations at each end of 50 Ω. Assume that the attenuation should be 30 dB or more at frequencies separated by a factor of 2 from the cutoff. We see from Table 2.2 that a fifth order filter is good enough to provide the needed attenuation. The normalized component values are $g_1 = g_5 = 0.618$, $g_2 = g_4 = 1.618$ and $g_3 = 2.000$. The filters are designed using this data with the preceding equations.

The resulting filters are shown in Fig. 2.20. The low pass is designed with a

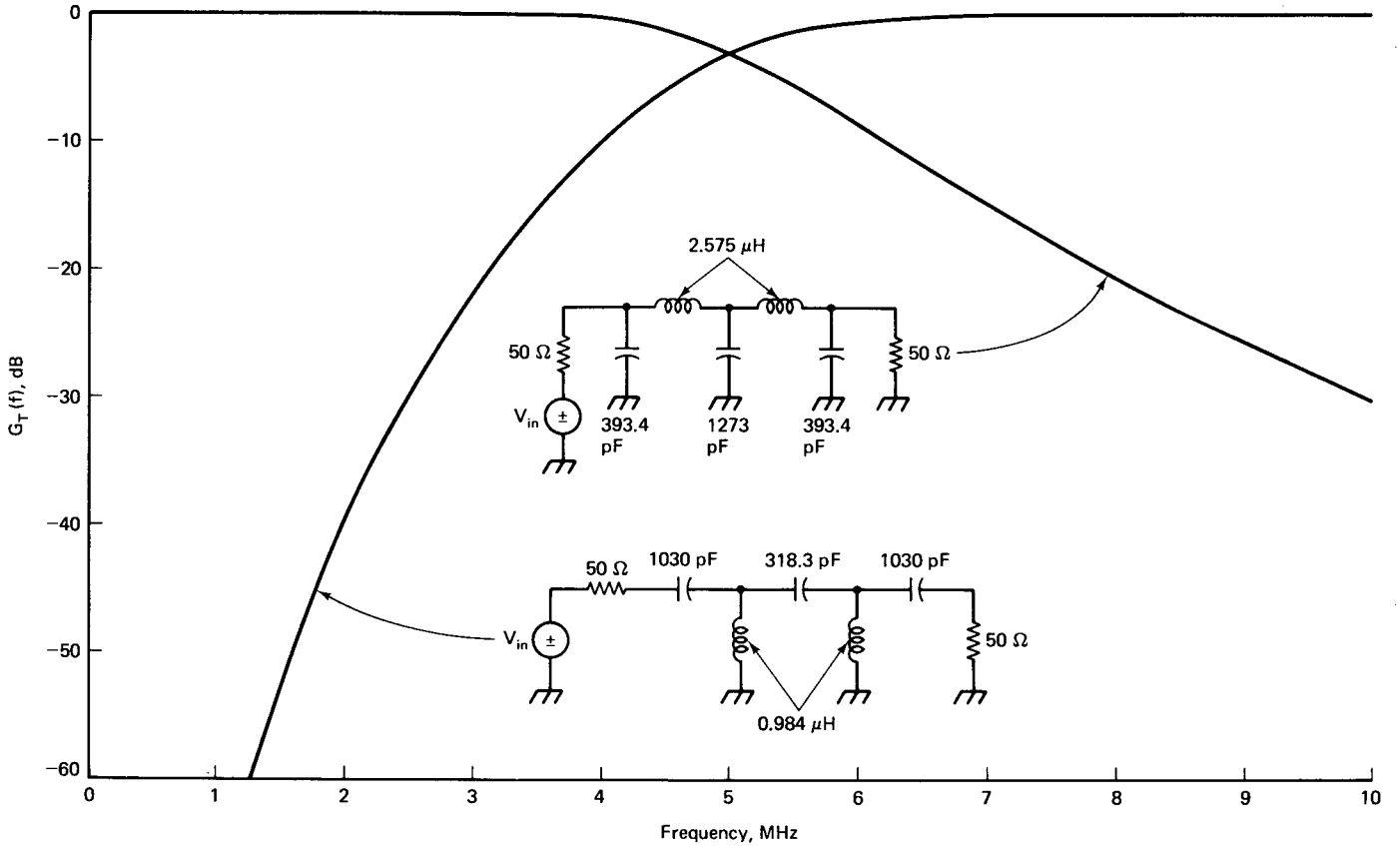

Figure 2.20 Circuits and frequency responses for five-pole low pass and high pass filters, each with a 5-MHz cutoff frequency. The frequency response curves would be absolutely symmetrical about the cutoff frequency if a logarithmic frequency scale was used.

shunt capacitor as the input element while the high pass uses a series capacitor at the input. The transducer gain of each is also presented in the figure. They were obtained with the ladder method of analysis.

The duals of the filters of Fig. 2.20 are presented in Fig. 2.21. The choice of the type to build is purely arbitrary. It will depend upon the application and the practicality of the components.

The low pass filter is the mirror image of the high pass although it may not appear so from the curves of Fig. 2.20. Recall that normalized data are presented in terms of frequency ratios. The cutoff of each of the filters in Fig. 2.20 is 5 MHz. The low pass is 30 dB down at twice this value, 10 MHz. Similarly, the high pass is 30 dB down at half the cutoff, or 2.5 MHz.

The transfer functions of the two filters will differ significantly. The low pass will be an all-pole function. However, the high pass filter will show zeros. Still, the high pass structure is usually termed a five-pole filter, for it resulted from denormalization of a five-pole low pass.

A simple bandpass filter is designed with little more effort than a low pass. The procedure is straightforward. First, the two band edges are determined. The difference is the bandwidth. The center frequency is the geometric mean of the two edges

$$f_{\text{center}} = (f_1 f_2)^{1/2} \tag{2.8-5}$$

where f_1 and f_2 are the passband edges. A low pass filter is first designed with a bandwidth equaling that of the desired bandpass filter. Then, the resulting low pass elements are resonated with the addition of components at the center frequency of the filter as given by Eq. 2.8-5.

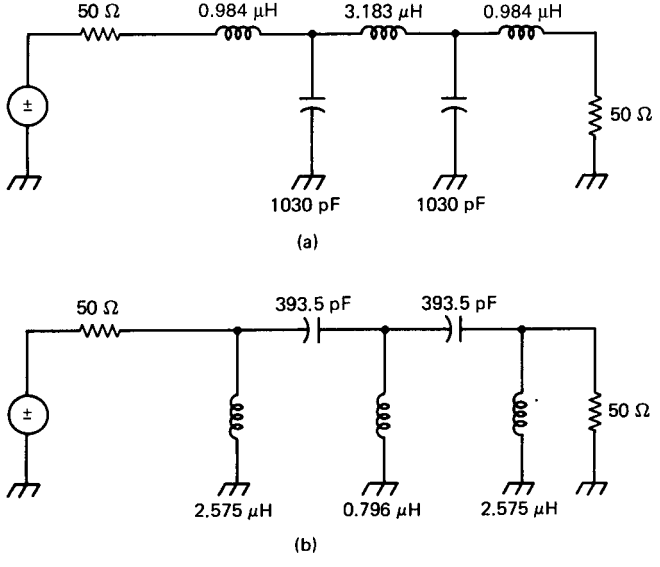

Figure 2.21 The dual forms of the 5-MHz cutoff filters of Fig. 2.20.

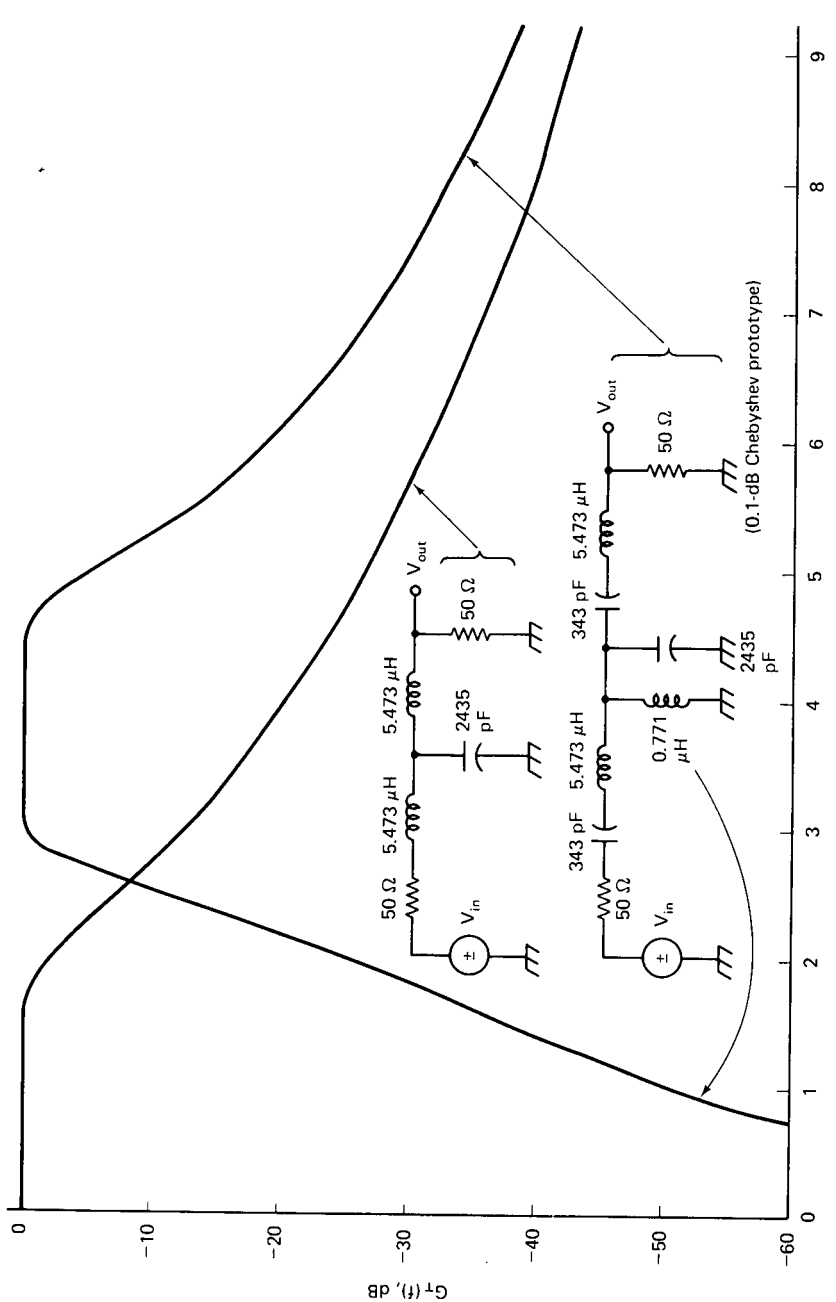

Figure 2.22 Circuits and frequency responses for a 1.5-MHz cutoff low pass filter and a bandpass filter with a 1.5-MHz bandwidth. The bandpass circuit is realized by resonating the elements of the low pass at the desired center frequency.

Assume that a bandpass filter is to be built to cover the range from 3 to 4.5 MHz and that the variation in response within the passband should not vary more than 0.1 dB. Assume also that stopband requirements are consistent with a third order Chebyshev filter and a 50-Ω termination is needed. The resulting filter design is shown in Fig. 2.22. From Table 2.1, a low pass filter with an 0.1-dB Chebyshev response is designed. The series inductors are then resonated at 3.674 MHz with series capacitors while the parallel capacitor is tuned with an appropriate parellel inductor. The result is the desired bandpass filter. Both low pass and bandpass responses and both circuits are given in Fig. 2.22.

This bandpass filter lacks arithmetic symmetry. If needed, this is approximated by cascading a suitable low pass filter with a cutoff equal or just higher than the upper cutoff of the bandpass structure.

The transfer function of the bandpass filter will contain both poles and zeros. Where the low pass prototype had three poles, this filter has six. They will occur in two bunches arranged as points on ellipses. The ellipses are centered about the positive and negative points in the s plane corresponding to the center frequency of the filter.

Even though this filter has six poles in its response, it is still a three-pole bandpass filter. It has three pole pairs and is derived from a three-pole low pass prototype. Generally, bandpass filters described by the number of poles are really being described by the number of resonators in the filter.

This method of bandpass synthesis is generally limited to wide bandwidths, usually 10% of the center frequency or more. In addition, the component values that are encountered are sometimes much less than practical. Methods for the design of narrower bandpass filters are presented in the next chapter.

The Chebyshev examples presented have been denormalized on the basis of the edge of the ripple band. Assume that it is desired to build a filter with a Chebyshev response, but with a well-defined 3-dB bandwidth. This is done by modifying the normalized component values. The key is the 3-dB frequency, which has been evaluated for the g_k values shown in Table 2.1. The g_k values are all multiplied by the normalized 3-dB frequency. The resulting filter will then have the same response as the original, but will have 3 dB of attenuation at 1 rad s^{-1}. The new normalized g_k results are then used in the denormalization equations.

The designer using any of the many collections of tabulated data should be careful to ascertain the form of that data. The extensive tables and graphs presented by Zverev are all normalized to a 3-dB cutoff frequency of 1 rad s^{-1}, making comparisons more direct.

REFERENCES

1. Van Valkenburg, M. E., *Network Analysis,* 3rd ed., Prentice-Hall, Englewood Cliffs, N.J., 1974.
2. Skilling, Hugh Hildreth, *Electric Networks,* John Wiley & Sons, New York, 1974.

3. Blinchikoff, Herman J. and Zverev, Anatol I., *Filtering in the Time and Frequency Domains,* John Wiley & Sons, New York, 1976.
4. Band, William, *Introduction to Mathematical Physics,* D. Van Nostrand, Princeton, N.J., 1959.
5. Johnson, D. E., Hilburn, J. L., and Johnson, J. R., *Basic Electric Circuit Analysis,* Prentice-Hall, Englewood Cliffs, N.J., 1978.
6. Ramo, Simon, Whinnery, John R., and Van Duzer, Theodore, *Fields and Waves in Communication Electronics,* John Wiley & Sons, New York, 1965.
7. DeMaw, M. F., *Ferromagnetic-Core Design and Application Handbook,* Prentice-Hall, Englewood Cliffs, N.J., 1981.
8. See reference 3.
9. Zverev, Anatol I., *Handbook of Filter Synthesis,* John Wiley & Sons, New York, 1967.